LIMNOLOGY
and
OCEANOGRAPHY

ASLO

*Limnol. Oceanogr.* 00, 2017, 00–00

doi: 10.1002/lno.10519

# From polar night to midnight sun: Diel vertical migration, metabolism and biogeochemical role of zooplankton in a high Arctic fjord (Kongsfjorden, Svalbard)

**G. Darnis,[1]* L. Hobbs,[2] M. Geoffroy,[3,4] J. C. Grenvald,[5] P. E. Renaud,[1,5] J. Berge,[4,5] F. Cottier,[2,4] S. Kristiansen,[4] M. Daase,[4] J. E. Søreide,[5] A. Wold,[6] N. Morata,[1] T. Gabrielsen[5]**

[1]Akvaplan-niva. Fram Centre for Climate and the Environment, Tromsø, Norway
[2]Scottish Association for Marine Science, Oban, United Kingdom
[3]Université Laval, Pavillon Alexandre-Vachon, Québec, Québec, Canada
[4]Faculty of Biosciences, Fisheries and Economics, UiT The Arctic University of Norway, Tromsø, Norway
[5]University Centre in Svalbard, Longyearbyen, Norway
[6]Norwegian Polar Institute, Tromsø, Norway

## *Abstract*

Zooplankton vertical migration enhances the efficiency of the ocean biological pump by translocating carbon (C) and nitrogen (N) below the mixed layer through respiration and excretion at depth. We measured C and N active transport due to diel vertical migration (DVM) in a Svalbard fjord at 79°N. Multifrequency analysis of backscatter data from an Acoustic Zooplankton Fish Profiler moored from January to September 2014, combined with plankton net data, showed that *Thysanoessa* spp. euphausiids made up > 90% of the diel migrant biomass. Classical synchronous DVM occurred before and after the phytoplankton bloom, leading to a mismatch with intensive primary production during the midnight sun. Zooplankton DVM resulted in C respiration of 0.9 g $m^{-2}$ and ammonium excretion of 0.18 g N $m^{-2}$ below 82 m depth between February and April, and 0.2 g C $m^{-2}$ and 0.04 g N $m^{-2}$ from 11 August to 9 September, representing > 25% and > 33% of sinking flux of particulate organic carbon and nitrogen, respectively. Such contribution of DVM active transport to the biological pump in this high-Arctic location is consistent with previous measurements in several equatorial to subarctic oceanic systems of the World Ocean. Climate warming is expected to result in tighter coupling between DVM and bloom periods, stronger stratification of the Barents Sea, and northward advection of boreal euphausiids. This may increase the role of DVM in the functioning of the biological pump on the Atlantic side of the Arctic Ocean, particularly where euphausiids are or will be prevalent in the zooplankton community.

The World Ocean plays a critical role in the mitigation of the planetary greenhouse effect due to $CO_2$ by absorbing about one third of the anthropogenic emissions of carbon to the atmosphere (Marinov and Sarmiento 2004). The oceanic uptake of $CO_2$ is regulated by physical and chemical processes, referred to as the "solubility pump," and a complex set of biological processes known as the "biological pump" (Ducklow et al. 2001). The mechanics of the latter involve the fixation of inorganic carbon by phytoplankton photosynthesis in the photic layer and subsequent vertical translocation of pelagic new primary production, either by sinking (passive or sinking flux) or transport (active flux), to depth below a pycnocline (Longhurst and Harrison 1988; Steinberg et al. 2000; Steinberg et al. 2002).

In the temperate and tropical ocean, extensive diel vertical migration (DVM) of zooplankton and micronekton has been shown to play a significant role in the vertical flux of particulate and dissolved organic matter (Longhurst et al. 1990; Steinberg et al. 2002; Takahashi et al. 2009). Active transport can represent up to 70% and 82% of the sinking fluxes of particulate organic carbon (POC), and nitrogen (PON), respectively (Dam et al. 1995). Typically, herbivorous zooplankton feed in the epipelagic layer at night and migrate to depth before dawn to avoid predation by visual predators (Brierley 2014). There they release carbon and nitrogen during egestion, and as $CO_2$ and $NH_4^+$ through respiration and excretion (Bronk and Steinberg 2008; Steinberg et al. 2008).

*Correspondence: Gerald.Darnis@akvaplan.niva.no

Additional Supporting Information may be found in the online version of this article.

In Arctic ecosystems, the high seasonality in light climate, shifting between the "polar night" (when the sun remains below the horizon) and "midnight sun" (when the sun does not set for extended periods) seasons makes zooplankton DVM responses more complex than at lower latitudes (Ringelberg 2010; Last et al. 2016). The rapid changes in day-night cycle and other environmental factors affect timing, synchrony, and vertical range of migration (Fischer and Visbeck 1993; Berge et al. 2014), which in turn influence the transport potential over the year. In such a variable light environment, snapshot sampling during scientific cruises limits the assessment of the consequences of zooplankton DVM. However, studies using multi-month time-series of acoustic data from moored instruments have shed light on the seasonal patterns of DVM. Acoustic Doppler current profilers (ADCPs) have recorded periods where zooplankton behavior resembles classical DVM, when the relative rate of change in irradiance is sufficient to trigger synchronous movements of zooplankton in winter-spring and autumn. The data have also suggested unsynchronized (individual) vertical movements under the continuous illumination of the Arctic summer when algal food is usually plentiful in the surface layer (Cottier et al. 2006; Berge et al. 2009; Wallace et al. 2010). Plankton-net data, sometimes combined with acoustic data, have shown that euphausiids, hyperiid amphipods, large *Calanus* and *Metridia* copepods, chaetognaths, and ctenophores are the main diel migrants in Arctic waters, their relative importance fluctuating with seasons and locations (Fischer and Visbeck 1993; Fortier et al. 2001; Daase et al. 2008; Berge et al. 2014).

One study based on a 10-month analysis of zooplankton in the southeastern Beaufort Sea revealed the importance of seasonal vertical migration (SVM) for carbon budgets in Arctic systems (Darnis and Fortier 2012). Carbon export below 200 m depth, mediated by large seasonal migrants such as the Arctic copepods *Calanus hyperboreus* and *Calanus glacialis* that overwinter at depth, was found to be of the same magnitude as the annual sinking POC flux measured by sediment traps. The impacts of both the well-known DVM taking place during the lighted season (Cottier et al. 2006; Wallace et al. 2010) and the recently discovered DVM during polar night (Berge et al. 2009; Wallace et al. 2010), however, have not been estimated. It is likely that ongoing DVM by some components of the community during winter will add to the proportion of vertical flux during this season accounted for by SVM. The consequences of DVM for the biological pump around the time of maximum new production are difficult to predict, however. This information is needed if we are to forecast the response of the Arctic marine ecosystem to the rapid warming of its waters and potential alteration of timing of ecological processes and the faunal assemblages present (Ardyna et al. 2014).

Here, we document the effect of synchronous DVM on the export to depth of carbon and nitrogen, using a 7-month time series of acoustic data collected with a moored acoustic zooplankton fish profiler (AZFP) in combination with plankton-net sampling in a high-Arctic Svalbard fjord, Kongsfjorden. In particular, we measure remineralization of carbon through respiration and excretion of ammonium at depth and assess the importance of the active transport relative to other fluxes.

## Methods

### Environmental setting of the study area

Sampling was carried out at or in the vicinity of station KB3 (78°57′N, 11°56′E, ca. 320 m depth) in the outer basin of Kongsfjorden (Fig. 1). Located on the west coast of Spitsbergen, Svalbard archipelago, Kongsfjorden is a wide glacial fjord consisting of two main basins separated by a 30-m deep sill (Svendsen et al. 2002). Three large tidewater glaciers calve into the relatively shallow inner basin (< 80 m depth), providing the main source of freshwater to the fjord (Cottier et al. 2005). Seaward, a submarine glacial trench (Kongsfjordrenna) connects the deeper (< 400 m depth) outer basin of Kongsfjorden to the West Spitsbergen Shelf and allows relatively free water-mass exchange across the shelf-fjord boundary. The fjord is therefore largely influenced by advection of both warm, saline Atlantic Water from the West Spitsbergen Current and colder, fresher Arctic water originating from the more coastal East Spitsbergen Current (Fig. 1) (Svendsen et al. 2002; Cottier et al. 2005). The Kongsfjorden zooplankton assemblage, a mixture of boreo-Atlantic and Arctic species, reflects the dual influence of these water masses (Kwasniewski et al. 2003; Basedow et al. 2004; Willis et al. 2006). The fjord has remained essentially ice-free since a major inflow of Atlantic Water during the winter of 2005–2006 (Cottier et al. 2007). In winter, the entire water column is homogeneous (Fig. 2) but a strong pycnocline forms during the summer months, as a result of strong freshwater discharge due to glacial and snow melt (Cottier et al. 2010).

The light regime in Kongsfjorden, at 79°N, is characteristic of high latitude regions with the sun remaining more than 6° below the horizon from 10 November to 1 February, the so-called "polar night" period (Berge et al. 2015). In contrast, the "midnight sun" period extends from 18 April to 23 August when the sun does not set below horizon.

Timing of the spring phytoplankton bloom in Kongsfjorden is variable and dependent upon physical factors, such as light levels, occurrence of sea ice inside and outside the fjord, and mixing processes, (Hegseth and Tverberg 2013). Usually, the spring bloom takes place between mid-April and late May (Seuthe et al. 2011; Hodal et al. 2012; Hegseth and Tverberg 2013).

### Acoustic sampling and data analysis

Several moorings were deployed over the course of 2013–2014 at a short distance from sampling station KB3 (Fig. 1). The instruments fitted on the moorings are detailed in Table

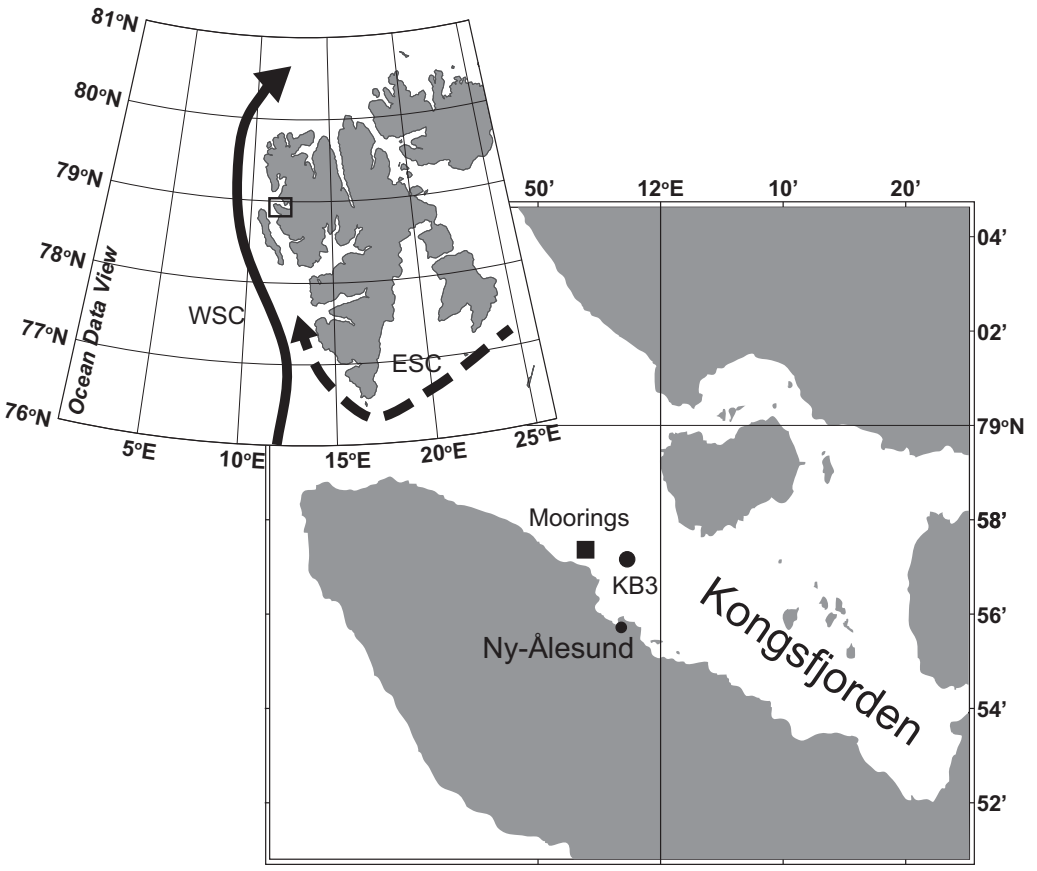


**Fig. 1.** Location of the sampling station KB3 in Kongsfjorden and of three moorings; one with an AZFP, one with two ADCPs, and another with fluorescence and PAR sensors (Table 1) The northward flowing West Spitsbergen Current (WSC; black arrow) and East Spitsbergen Current (ESC; dashed arrow) are illustrated.

1. On one of the moorings, an upward-looking Acoustic Zooplankton Fish Profiler™ (AZFP; ASL Environmental Science, Victoria, Canada) continuously recorded hydroacoustic data at 125 kHz, 200 kHz, 455 kHz, and 769 kHz from 17 January to 9 September 2014. Since the 769 kHz transducer only insonified a water layer of a few meters above the instrument, data from only the three lower frequencies were considered in this study. The AZFP was moored at 84 m within a stainless steel frame supported by floats. To limit the backscatter from other moored instruments located higher on the mooring line, the AZFP was mounted with an 8° angle relative to the vertical mooring line. The vertical angle, the pitch and roll of the AZFP were taken into account in the internal beam-mapping algorithm of the AZFP to assign real depths to mean volume backscattering strength (Sv in dB re 1 $m^{-1}$) and target strength (TS in dB re 1 $m^{-2}$) values. Vertical resolution varied from 23.6 cm at 455 kHz to 98.4 cm at 125 kHz. The pulse duration and nominal beam angle also varied with the frequency (Supporting Information Table S1). Source level was 210 dB (re 1$\mu$Pa at 1 m) and ping rate was 1 ping·10 $s^{-1}$ (0.1 Hz) from 17 to 22 January and 0.05 Hz thereafter. The AZFP was calibrated by the manufacturer (± 1 dB) prior to deployment (ASL 2014).

Acoustic data were processed with EchoView® 6.0. Bad pings, the backscatter from the sediment trap, the top two meters of the water column and the first two meters nearest to the AZFP were excluded from the analysis. Strong echoes typical of fish schools (Supporting Information Fig. S1) were also removed from the echograms to keep only the signal from zooplankton. The monthly echogram at each frequency was divided into 1-m vertical by 5-min horizontal echo-integration cells and mean Sv within each cell was exported.

Scattering models can be used to predict the acoustic response of scatterers to specific frequencies (Stanton et al. 1998). This response varies between types of zooplankton (or functional groups) due to changes in body shape, size, orientation, and the contrast in density and sound speed between scatterers and the surrounding water (Kristensen and Dalen 1986; Lawson et al. 2004). Net samples from Kongsfjorden in January 2014 showed the most numerically dominant functional groups to be copepods, euphausiids, and chaetognaths. These three groups can all be modeled as fluid-like

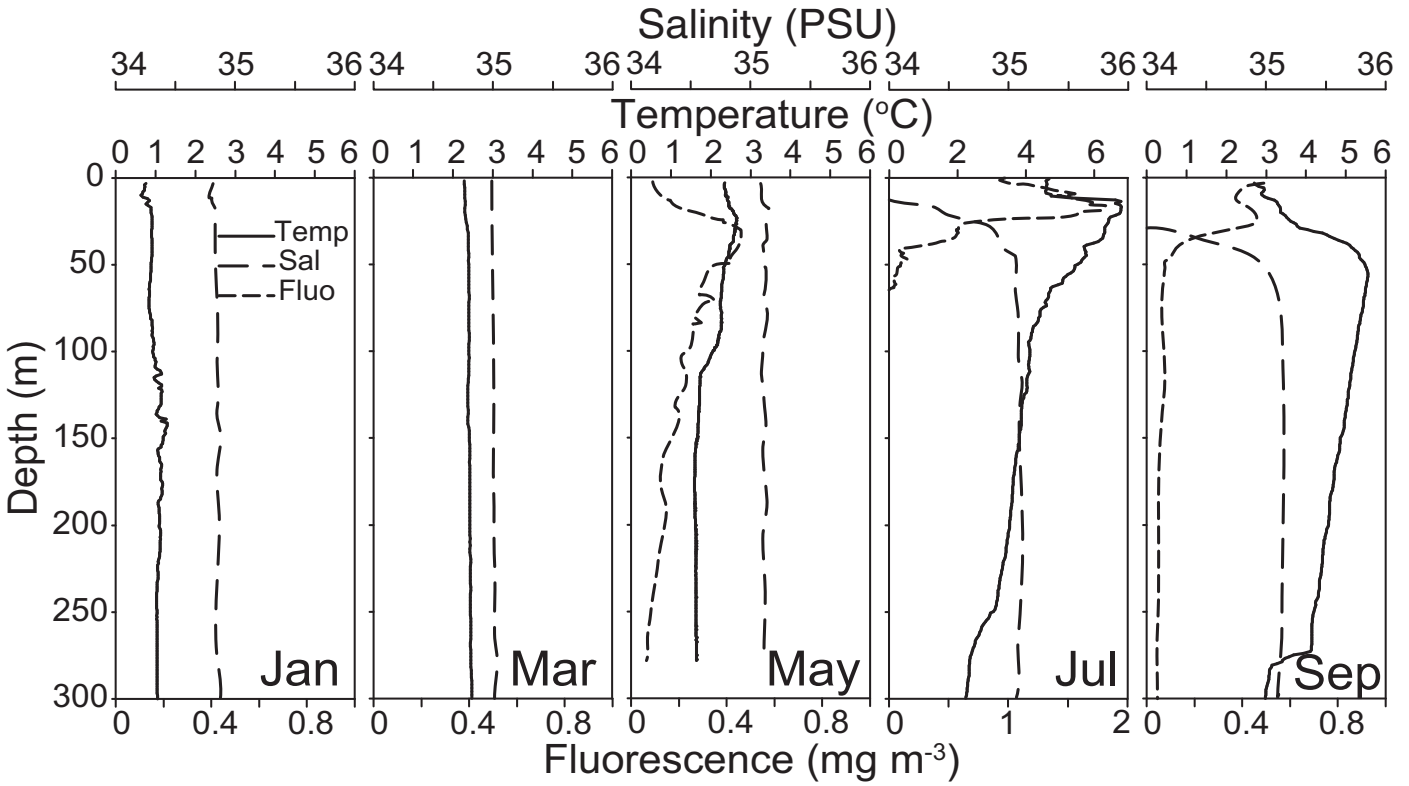


**Fig. 2.** Vertical profiles of temperature, salinity, and fluorescence at station KB3 in Kongsfjorden at different dates of 2014.

**Table 1.** Positions, periods of deployment, and details on the moored instruments in Kongsfjorden used in the present study.

| Mooring | Bottom depth (m) | Latitude | Longitude | Deployed | Recovered | Instrumentation |
|---|---|---|---|---|---|---|
| AZFP 1 | 203 | 78°57.49′N | 11°49.25′E | 17 Jan 2014 | 09 Sep 2014 | Upward AZFP 84 m |
| | | | | | | Sediment trap 40 m |
| ADCP 1 | 231 | 78°57.76′N | 11°47.93′E | 23 September 2014 | 25 September 2014 | Downward ADCP 96 m |
| | | | | | | Upward ADCP 95 m |
| | | | | | | Sediment trap 65 m |
| ADCP 2 | 236 | 78°57.75′N | 11°48.30′E | 05 Oct 13 | 09 Sep 2014 | ADCP 108 m |
| | | | | | | ADCP 102 m |
| | | | | | | Sediment trap 100 m |
| | | | | | | Sediment trap 50 m |
| | | | | | | Fluor. sensor 37 m |
| | | | | | | PAR sensor 37 m |
| ADCP 3 | 243 | 78°57.73′N | 11°48.43′E | 01 Oct 2012 | 06 Sep 2013 | ADCP 108 m |
| | | | | | | ADCP 102 m |
| | | | | | | Sediment trap 105 m |
| | | | | | | Sediment trap 50 m |
| | | | | | | Fluor. sensor 38 m |
| | | | | | | PAR sensor 38 m |

weak scatterers (Stanton and Chu 2000) using the Distorted Wave Born Approximation approach (Stanton et al. 1998). Scattering models were fitted for each functional group using a range of sizes (Supporting Information Table S2) and specific orientation angles for copepods (Benfield et al. 2000), euphausiids (Chu et al. 1993) and chaetognaths (Fredrika Norrbin; unpubl. Video Plankton Recorder data from Kongsfjorden), at the three frequencies of the AZFP.

These models demonstrated that euphausiids have a frequency response of $Sv_{125kHz} > Sv_{200kHz} < Sv_{455kHz}$; copepods of $Sv_{125kHz} < Sv_{200kHz} < Sv_{455kHz}$; and chaetognaths $Sv_{125kHz} < Sv_{200kHz} > Sv_{455kHz}$. Using these differences in the frequency responses, each echo-integration cell was partitioned into one of the three functional groups, which was assumed to be dominant within that given cell.

Mean TS for each functional group was then estimated based on the randomly oriented fluid bent cylinder model (Stanton et al. 1994). The average dry weight $W$ of individual euphausiids and copepods was estimated from measurements of individuals made on a microbalance whereas the $W$ of chaetognaths was estimated using a length-dry weight relationship established for *Parasagitta elegans* (Welch et al. 1996) (Supporting Information Table S2). Mean dry biomass (mg $m^{-3}$) within each echo-integration cell associated with euphausiids (Eq. 1), copepods (Eq. 2), or chaetognaths (Eq. 3) was calculated following Parker-Stetter et al. (2009):

$$\text{Biomass}_{\text{euphausiids}} = \left(\frac{s_{v125kHz}}{\sigma_{\text{bseuphausiids}}}\right) \cdot W_{\text{euphausiids}} \quad (1)$$

$$\text{Biomass}_{\text{copepods}} = \left(\frac{s_{v455kHz}}{\sigma_{\text{bscopepodss}}}\right) \cdot W_{\text{copepods}} \quad (2)$$

$$\text{Biomass}_{\text{chaetognaths}} = \left(\frac{s_{v200kHz}}{\sigma_{\text{bschaetognaths}}}\right) \cdot W_{\text{chaetognaths}} \quad (3)$$

Where $s_v$ is the linear volume backscattering strength ($m^2$ $m^{-3}$), $\sigma_{bs}$ is the expected backscattering cross-section of an element of the zooplankton group ($m^{-2}$), and $W$ is the average dry weight (mg). The biomass of each zooplankton group was integrated in the top 2–40 m (above the trap) and 2–82 m layers and averaged for each month during the day and the night hours. Day was defined as the time-interval of minimum backscatter in the targeted water layer around local midday measured on the echogram at 125 kHz of the AZFP (Supporting Information Fig. S2), whereas night was the period of higher backscatter during the remainder of the 24-h cycle. Dry biomass was converted to carbon content using the C : $W$ factor of 0.5189, 0.5366, and 0.3844 for euphausiids (i.e., *Thysanoessa inermis*), large copepods, and chaetognaths (i.e., *P. elegans*), respectively (Ikeda and Skjoldal 1989).

To gain insight into the zooplankton DVM patterns beyond the period sampled with the AZFP (until 9 September), additional acoustic data were obtained during a short-term mooring deployment close to the autumn equinox (23–25 September). The mooring was equipped with two 307-kHz RDI ADCPs, one upward-looking at 95 m, the other downward-looking at 96 m. In addition, a Parflux 21-cup sediment trap was positioned at 65 m to intercept sinking particles and zooplankton swimmers (Table 1). The ADCPs measured the mean echo strength from ensembles of 60 pings at a rate of 1 ping $s^{-1}$ in 22 depth layers (bins of 4 m). The raw echo intensity data were converted to a measure of absolute volume backscatter (Sv, in dB) (Berge et al. 2014). The ADCPs would detect zooplankton of the size of medium to large *Calanus* copepodite stages (> 5 mm of prosome length) and larger.

A Seapoint fluorometer and photosynthetic active radiation (PAR) sensor, both mounted at 37 m depth on an adjacent mooring, provided raw fluorescence and PAR data in the vicinity of station KB3 from 5 October 2013 to 9 September 2014.

**Ship-based sampling and taxonomic analysis**

Net sampling for macro- and meso-zooplankton was carried out at station KB3 using R/V *Helmer Hanssen* from 16 to 20 January and 23 to 27 September 2014. Additional mesozooplankton samples were taken between 12 and 14 May, using the workboat *Teisten*, and on 23 July using R/V *Lance*. Macrozooplankton was sampled as close as possible to local midday and midnight by trawling obliquely from 30 m depth to the surface at two knots for approximately 5–10 min with a Methot-Isaac-Kidd (MIK) ring net (3.15 $m^2$ aperture, 13-m long net with 1500 $\mu$m mesh size, and a 500 $\mu$m mesh in the last meter), fitted with a 10-L cod end and equipped with a Hydrobios flowmeter at the center of the ring. Upon retrieval, the zooplankton samples were subdivided and 2/3 to 3/4 of the cod end was fixed in a borax-buffered seawater solution of 4% formaldehyde for taxonomic identification. Nine and four MIK net deployments were done in January and September, respectively.

Mesozooplankton was sampled around midday and midnight, using a Hydro-Bios multiple plankton sampler Midi-MultiNet (0.25 $m^2$ aperture, 5 nets of 200-$\mu$m mesh) hauled vertically at 0.5 m $min^{-1}$. The sample depths were 320–200 m, 200–100 m, 100–50 m, 50–20 m, and 20–0 m depth. In May, successive deployments of a KC Denmark WP2 net (0.25 $m^2$ aperture, 200-$\mu$m mesh) with a closing system were done instead of the MultiNet sampling, and the deepest stratum sampled reached 300 m depth. No replicate sampling of each depth stratum was performed. Upon collection, the content of the cod ends was preserved in seawater solution of 4% hexamethylen-buffered formaldehyde for taxonomic identification. Four MultiNet deployments were performed in January, three in May, one in July, and four in September. CTD (Seabird SBE 911) casts through the water column were carried out immediately before or after net deployments to collect profiles of temperature, salinity, and fluorescence.

In January, May, and September, additional MIK and MultiNet/WP2 casts were carried out at station KB3 to catch live zooplankton for respiration, ammonium excretion, and biomass measurements. The sampling using a WP2 or WP3 (1 $m^2$ aperture, 1000-$\mu$m mesh) net was performed on the Svalbard shelf from 18 to 28 May for mesozooplankton respiration measurement onboard *Helmer Hanssen*. Each net of the samplers was fitted with a rigid cod end with filtration

apertures at the top of the cylinder to keep the animals in sufficient water until collection. Upon retrieval, each sample was diluted in cold filtered (0.2–0.7 $\mu$m GF/F) seawater and any large jellyfish were removed. Other macrozooplankton such as amphipods, euphausiids, and *Clione limacina* were also removed from the samples collected with the MultiNet/WP2 to avoid predation and stress on the mesozooplankton size class. The live samples were kept in the dark in a temperature-controlled room set at close to in situ temperature (1–4°C) until further treatment.

In the laboratory, known aliquots (up to 1/8) were taken from the MIK formalin-preserved macrozooplankton samples and all non-copepod organisms were counted and identified to species level under a stereomicroscope before measuring their total body length. Samples from the MultiNet casts were size-fractionated on a 1000-$\mu$m sieve and re-suspended in distilled water. Successive known aliquots were taken from the 200-$\mu$m to 1000-$\mu$m fraction with a 5-mL large tip ($>$ 5 mm diameter) automatic pipette until 300 organisms were counted and identified to developmental stage and species, or to the lowest possible taxonomic level, under a stereomicroscope. The $>$1000-$\mu$m fraction was analyzed in its entirety. Prosome length of the *Calanus* copepodites was measured in both size-fractions.

### Zooplankton biomass, respiration, and ammonium excretion

Intact and active individuals of dominant macrozooplankton taxa, essentially *Thysanoessa* spp., *Themisto abyssorum*, and *Themisto libellula*, were rapidly sorted from the MIK live samples. A known subsample of each of the live samples collected with the MultiNet/WP2 was poured into a funnel fitted with a 1000-$\mu$m sieve inside and a gate valve to obtain two mesozooplankton size classes for incubation. The $>$1000-$\mu$m fraction was retained in the top part of the device in a sufficient volume of water while the 200–1000 $\mu$m small zooplankton was gently evacuated through the sieve through successive washes with cold oxygenated, filtered seawater. A sufficient number of macrozooplankton animals (1–10 depending on size and volume of incubation bottle) and each mesozooplankton size class were gently introduced in separate airtight glass bottles (110–280 mL capacity), which were thereafter filled with cold oxygenated filtered seawater and capped. Control bottles without zooplankton were made in triplicates for each experimental setup. Oxygen concentration was measured by optode respirometry with a 4-channel respirometer (Oxy-4 Mini, PreSens Precision Sensing GmbH, Regensburg, Germany) every 0.5–2 h for 8–12 h. Respiration rates were calculated by determining the slope of the decrease of oxygen over time and subtracting the mean value for the controls. Oxygen consumption rates were transformed to respiratory carbon using a respiratory quotient of 0.75 in January, assuming a winter metabolism mainly by lipid reserves (Ingvarsdóttir et al. 1999), and 0.97 from May onward with a metabolism primarily based on proteins (Gnaiger 1983).

Zooplankton ammonium ($NH_4^+$) excretion rate was estimated from the same incubations used for respiration and calculated as the difference in $NH_4^+$ concentration between incubation bottles and animal-free control bottles at the end of the experiment divided by the duration of incubation to obtain an hourly rate. In January, ammonium concentration was measured onboard immediately after collection while, in September, the water samples were preserved in acid-cleaned 125-mL polycarbonate bottles and immediately frozen. During the January and September fieldwork, triplicate samples of water were taken before the incubation for ammonium measurement. At termination of incubation, triplicate samples were retrieved from the incubation water. The ammonium samples were filtered through acid-washed Sartorius polycarbonate syringe filter holders equipped with preburned Whatman GF/C glass microfibre filters (6 h at 450°C). The filter holders were rinsed with deionized Milli-Q water before use. $NH_4$-N concentration was analyzed spectrofluorimetrically using a 5-cm cell following Solórzano (1969).

Right after the experiments organisms were carefully blotted on absorbent material and preserved in cryovials at −20°C. In the laboratory, the frozen samples were transferred to pre-weighed plastic cups, dried in an oven at 60°C for 48 h and then weighed on a microbalance ($\pm$ 1 $\mu$g). Carbon content (C) of each macro- and meso-zooplankton taxon was calculated from dry mass (*W*) measurements, using the specific C-*W* relationship in Ikeda and Skjoldal (1989).

### Active respiratory carbon and excretory nitrogen transport

To study the seasonal variation in zooplankton DVM patterns (spatial extent and strength in terms of biomass involved), and resulting active fluxes of carbon and nitrogen, the daily migrant biomass *MB* (mg C $m^{-2}$) of euphausiids, copepods, and chaetognaths was calculated. Monthly averages of migrant biomass integrated from surface to depth (z) over the 7-month time series were determined from Eq. 4:

$$MB_z = \int_z \text{night biomass} - \text{day biomass} \quad (4)$$

Transport out of the top 2–40 m and 2–82 m depth strata was considered. The lower limit of the layer (*z*) was set at 40 m depth for comparison of active transport with sinking flux measured with a sediment trap at that depth whereas *z* at 82 m corresponds to the maximum depth sampled with the AZFP.

The downward active transport at depth *z* was then calculated using Eq. 5:

$$AF_z = MB \times RE \times T \quad (5)$$

where *AF* is the active transport of carbon (mg C $m^{-2}$ $d^{-1}$) or nitrogen (mg N $m^{-2}$ $d^{-1}$) by migrant zooplankton, *RE* is

the specific hourly respiratory carbon loss (mg C mg $C^{-1}$ $h^{-1}$) or ammonium excretion (mg N mg $C^{-1}$ $h^{-1}$), and $T$ (h) is the time spent at depth during a 24-h cycle. $T$ was measured from the AZFP echogram at 125 kHz.

To calculate daily rates of community respiration, excretion and active transport due to DVM averaged over each month of the time-series, hourly specific metabolic rates of the different taxa and size classes had to be interpolated by using the three snapshot measurements of hourly rates of January, May, and late September to cover the whole study period. For mesozooplankton, we assumed that the size class- $>1000$ $\mu$m largely dominated by large copepods was primarily responsible for the backscatter recorded by the AZFP, and applied their specific hourly metabolic rates in the calculations. Chaetognath metabolic rates were not measured due to the difficulty of collecting undamaged individuals for incubations. Thus, we used a specific respiration of $0.40 \pm 1.06$ $\mu$g C mg $C^{-1}$ $h^{-1}$ and excretion of $0.15 \pm 0.12$ $\mu$g N mg $C^{-1}$ $h^{-1}$, measured by Ikeda and Skjoldal (1989) on *P. elegans*, the dominant chaetognath in Kongsfjorden.

## Sinking flux of POC and PON

To compare our estimates of active transport of carbon and nitrogen below the 40 m and 82 m depths with sinking fluxes of POC and PON, we analyzed samples from sequential automated sediment traps (McLane PARFLUX Mark78H; 0.66 $m^2$ collecting area; 21-cups turntable) deployed on moorings in Kongsfjorden (Table 1). A sediment trap at 40 m depth on the same mooring as the AZFP intercepted sinking particles from 21 January to 3 April 2014 at a sampling frequency of 3.5 d per cup. A large volume of terrigenous matter clogged a sediment trap at 100 m depth soon after deployment in October 2013, preventing from using the sediment samples to quantify sinking fluxes in the annual cycle 2013–2014. Therefore, we used the 2012–2013 time series of sediment samples to quantify POC and PON sinking at 100 m depth, assuming a low interannual variability in sinking fluxes outside of the bloom period.

Before deployment, the sample cups were filled with seawater filtered through Whatman GF/F 0.7 $\mu$m glass fiber filters, adjusted to 35 PSU with NaCl, and poisoned with formalin (2% v/v, sodium borate buffered). After recovery, zooplankton were removed from the samples using a dissecting microscope. Samples were then subdivided using a Motoda splitting box and filtered in triplicates through preweighed GF/F filters (25 mm diameter, 0.7 $\mu$m pore, precombusted for 4 h at 450°C). Filters were dried for 12 h at 60°C, weighed for dry weight and exposed to concentrated HCl fumes for 12 h to remove inorganic carbon. They were folded in tin cups that were then combusted in a EuroEA3022 elemental analyzer for measurement of POC and PON.

## Results

### Synchronous DVM

The continuous echogram of the AZFP at 125 kHz allows for the tracking of vertical distribution of scatterers over the 7-month period from the polar night to the end of summer. DVM behavior was identified qualitatively as periods of time where a strong scattering layer characterized by a strong band of green/red was seen to oscillate at a daily frequency over a depth range greater than 30 m (Fig. 3a). A clearly visible synchronous DVM extending below 40 m started on 28 January (Fig. 3b). From then on the depth range of the DVM signal increased, reaching 82 m on 31 January. This winter DVM persisted until 10 April (a few days before the onset of midnight sun), after which sporadic synchronous vertical movements did not usually occur in phase with the 24-h light cycle. Synchronous DVM resumed on 11 August, first with weak sporadic migrations (not every day), that reached a regular 24-h period in early September (Fig. 3c). Thus, classical DVM behavior occurred outside of the main season of primary production, between late May and late June in 2014 as shown by the fluorescence at 37 m depth (Fig. 3a). Strong echoes during the midnight sun in June and early July in the 2–82 m layer, indicative of strong zooplankton biomass but without evidence of classical DVM, coincided with this period of high biological production in the surface layer.

The echogram of the backscatter recorded by the ADCPs over 3 d in late September, 2 weeks after the end of the AZFP sampling, shows a strong DVM signal (Fig. 4). At midnight, the bulk of the backscatter was concentrated in the upper 20 m, whereas it was located between 120 m and 160 m at midday.

### Time spent at depth during a 24-h cycle

Time spent by scatterers below 40 m and below 82 m during a daily cycle showed a very similar strong linear increase from the start of DVM in late January to its end in April (Fig. 5). From early March onward, the small difference between times spent below 40 m and below 82 m indicated that the downward/upward migrations were swift from surface to below the two depth limits. From January to early March, zooplankton spent most of a diel cycle above 40 m or 80 m depth, with time at depth $<12$ h. Conversely, at the end of the late winter DVM period when there was more than 12 h of light per day, zooplankton were distributed below 82 m most of the day ($>20$ h). The same situation can be seen in late August and early September at the onset of the autumn synchronous DVM season.

### Composition of the migratory community from plankton net data

Macrozooplankton biomass in the surface 0–30 m layer estimated from the plankton net hauls tended to be slightly lower at midday than at midnight in January (Fig. 6). However, the low number of net deployments during each short

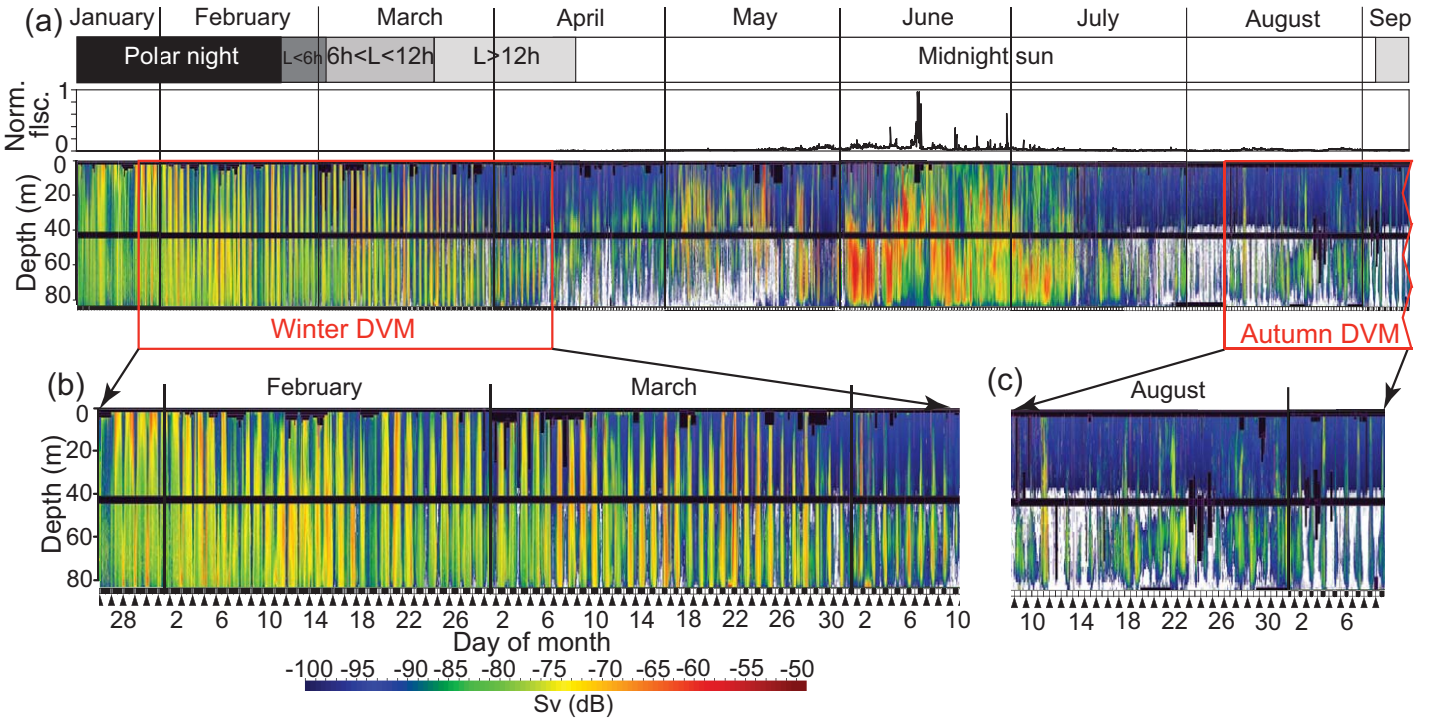


**Fig. 3.** (**a**) Time series of relative fluorescence (Norm. flsc.) at 37 m depth and backscatter for the 125 kHz frequency of the AZFP in Kongsfjorden from 17 January to 09 September 2014, and expanded views of (**b**) winter DVM period (28 January–10 April) and (**c**) onset of autumn DVM (10 August–09 September) defined qualitatively by visual analysis of the echogram.

cruise prevented the comparison of day and night zooplankton biomass for statistical differences. Extremely low biomass at midday at the surface compared to night was observed in September, indicating a strong DVM pattern. Euphausiids (mainly *T. inermis*, *T. raschii*, and *T. longicaudata*) represented 94% ± 4% of the macrozooplankton biomass at day and night in January and 91% ± 1% at night in September, but only 9% ± 3% of the day biomass in September. Chaetognaths (mainly *P. elegans*) contributed 5% ± 4% to the macrozooplankton biomass in January whereas they contributed 6% ± 3% of the biomass at night and 56% ± 16% at day in September when the biomass was extremely low. Contribution of the very few *Themisto* spp. to macrozooplankton biomass was negligible in January (< 0.01%) and low at night in September (< 3%). These amphipods represented, however, 30% of the very low surface macrozooplankton biomass at noon in September.

Mesozooplankton biomass in the surface 0–50 m layer did not show any difference between midday and midnight in January and May (Fig. 6). The biomass was lowest in May and highest in July, with *Calanus* spp. (*C. finmarchicus* and *C. glacialis*) dominating the mesozooplankton assemblage. These taxa, together with *C. hyperboreus* and *Metridia longa*, represented 69%, 68%, 92%, and 89% of the biomass at midday in January, May, July, and September, respectively, in the 0–50 m layer and 55% and 45% at midnight in January

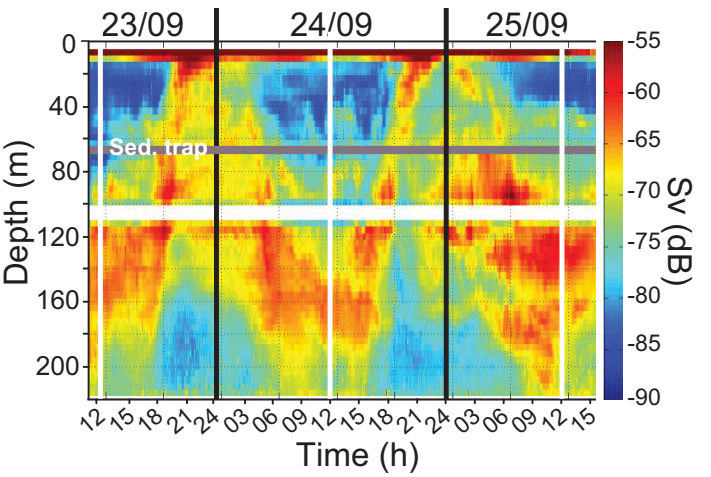


**Fig. 4.** Backscatter from two 307.2 kHz ADCPs, one upward-looking and the other downward-looking, from 23 to 25 September 2014 at the mooring site. Black and white vertical lines indicate local midnights and middays as per the clock.

and May. Newly hatched *T. abyssorum* contributed substantially to mesozooplankton biomass at midnight in May, thus reducing the relative importance of *Calanus* spp. Patterns in the 0–100 m layer were very similar to the ones described for the 0–50 m layer, except for an even higher discrepancy

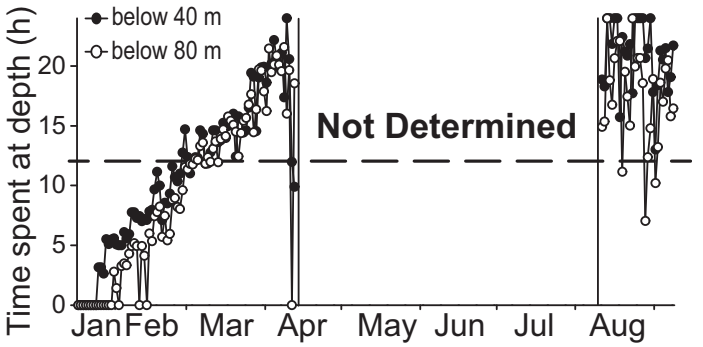


**Fig. 5.** Time series of time spent below 40 m and 82 m depth by the high backscatter over a 24-h cycle from January to September 2014. The horizontal broken line indicates the 12-h limit.

between day and night biomass in September (Fig. 6). The large copepods dominated the mesozooplankton biomass in roughly the same proportions as for the 0–50 m layer in the same months. The contribution of chaetognaths to mesozooplankton biomass never exceeded 5% in the two layers over the different months. In summary, evidence for strong DVM was essentially found in late September and the behavior was most pronounced for the macrozooplankton, particularly *Thysanoessa* spp.

### Diel migrant biomass from acoustic data

In the 2–40 m layer, the monthly mean of euphausiid biomass was always higher at night than at day from January to April, and from August to September (Fig. 7a). Euphausiid biomass showed a first peak in February, with 0.9 g C $m^{-2}$ at night, and a second peak of lesser magnitude in May–June during the midnight sun and peak season of primary production. The range of euphausiid biomass in January, estimated from the MIK net sampling a few days before the onset of synchronous DVM (0.09–0.6 g $m^{-2}$), is comparable with the range derived from the AZFP data for the entire study period (0.09–0.9 g $m^{-2}$). Likewise, night biomass estimates from the MIK nets close to the September equinox (0.5–0.8 g $m^{-2}$) were within the same range, whereas the estimates during the day were much lower (0.0008–0.001 g $m^{-2}$). The euphausiid migrant biomass, based on day-night change, peaked in February–March (> 0.6 g C $m^{-2}$) and reached a minimum in April (0.09 g C $m^{-2}$) close to the onset of midnight sun (Fig. 7b). The pattern in the 2–82 m layer was somewhat different from the observations in 2–40 m (Fig. 7c). First, the mean biomass was higher during day than at night in January, a bias likely due to DVM occurring essentially over the top 40 m layer until late January. The second peak of euphausiid biomass (3.2 g C $m^{-2}$) in the midst of midnight sun in June was higher than the first winter peak in March. Migrant biomass peaked in February–March, remaining above 1 g C $m^{-2}$.

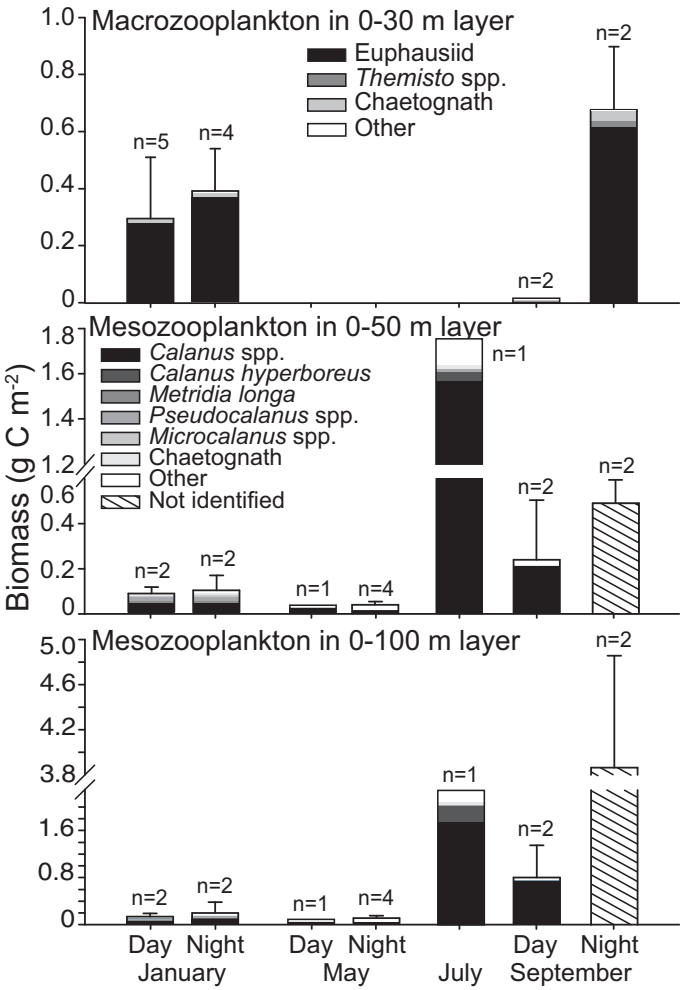


**Fig. 6.** Macro- and mesozooplankton biomass and composition from plankton net data in the surface 30-m, 50-m, and 100-m layer at day and at night in January, May, July, and September 2014 at station KB3 in Kongsfjorden. "n" indicates number of plankton net deployments.

Classical DVM was also observed for copepods and chaetognaths prior to the onset of midnight sun and in August–September in the 2–40 m layer (Figs. 8a, 9a). However, in the darkest months of January and February, copepod biomass tended to be higher at day than at night (Fig. 8a) and difference between night and day values was much less marked for the copepod group than for euphausiids and chaetognaths. On the other hand, the latter two displayed similar patterns, although the biomass estimates for the chaetognaths were much less.

Copepod and chaetognath biomass increased in the surface layer in June, coinciding with the season of high primary production. Copepod biomass from AZFP data (0.2–0.3 g $m^{-2}$) fell within the range of biomass values estimated from mesozooplankton net sampling of the top 0–50 m layer in January and September (0.02–0.2 g $m^{-2}$). For copepods, a classic migrant biomass (shallower distribution at night and

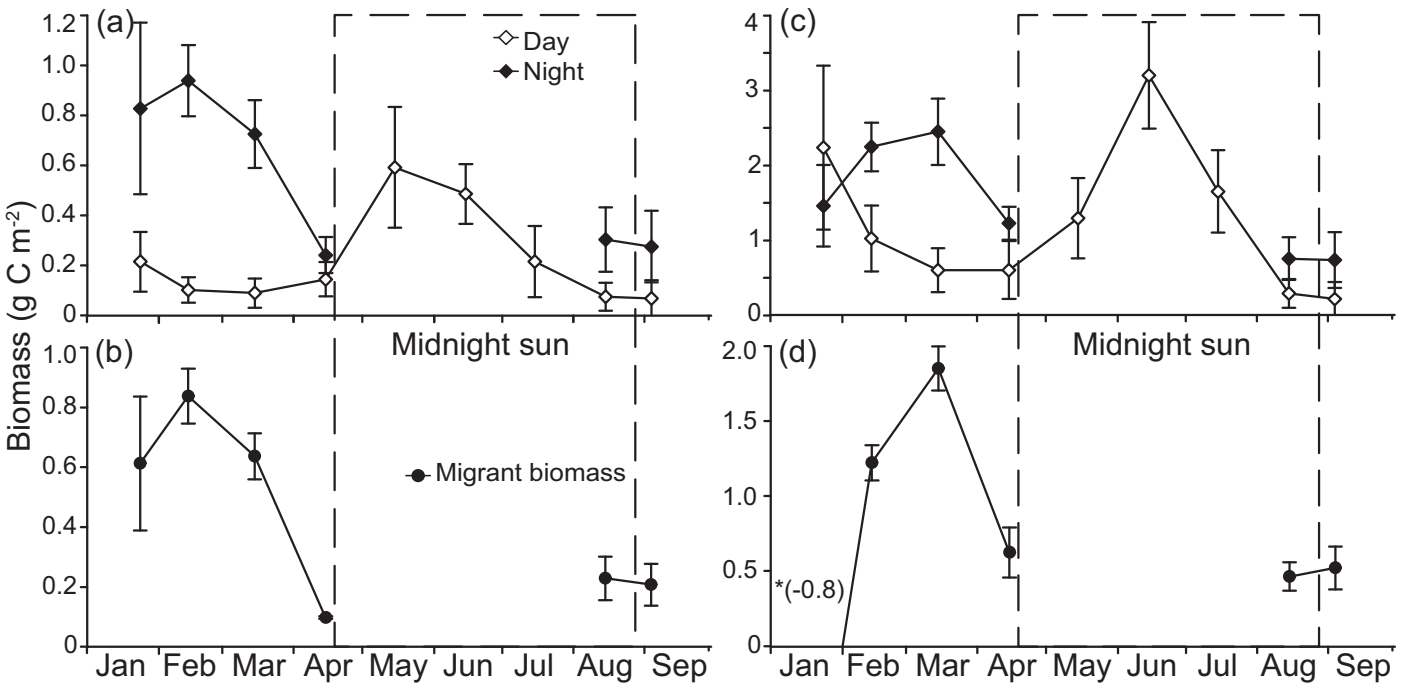


**Fig. 7.** Euphausiids. (**a** and **c**) time series of average monthly day and night biomass (± 1 SE) in the 40 m and 82 m above the AZFP, respectively, and (**b** and **d**) respective diel migrant biomass (± 1 SE) in the same layers, with *negative value indicating biomass during day higher than night. Note different scales on the y-axis among panels.

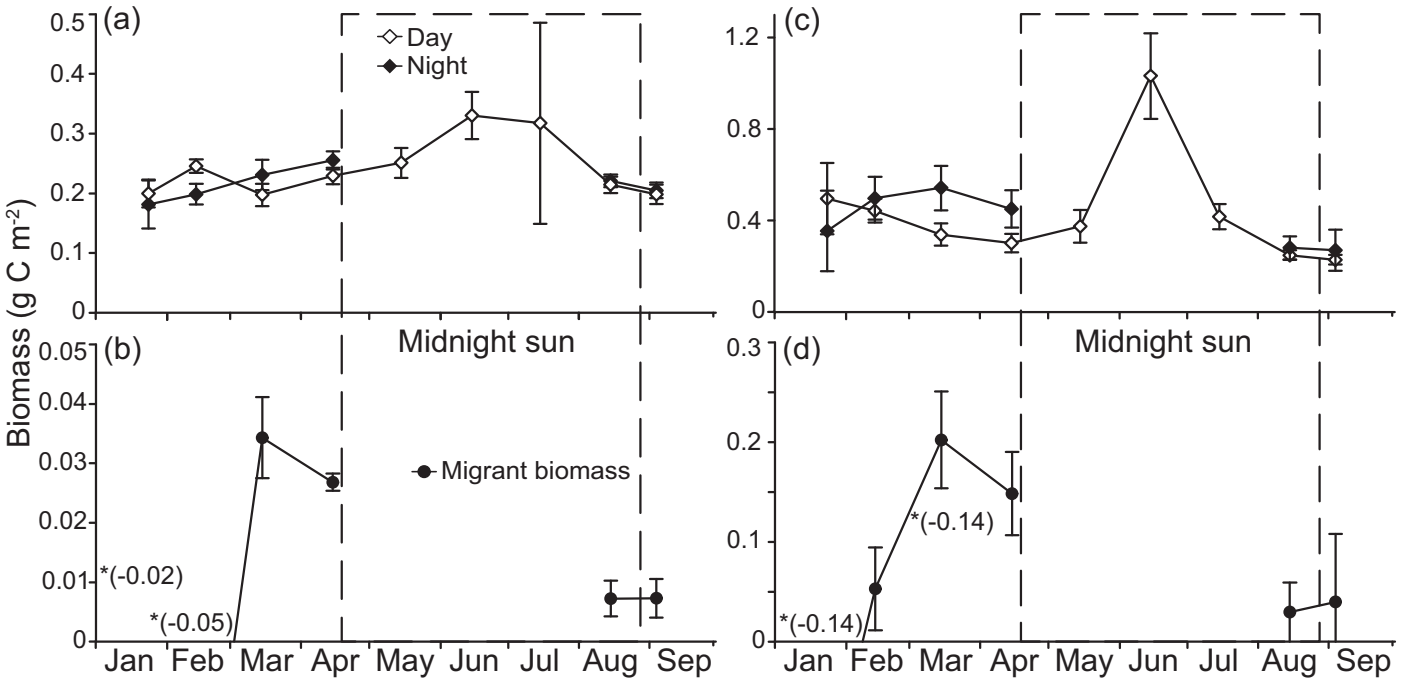


**Fig. 8.** Copepods. (**a** and **c**) time series of average monthly day and night biomass (± 1 SE) in the 40 m and 82 m above the AZFP, respectively, and (**b** and **d**) respective diel migrant biomass (± 1 SE) in the same layers, with *negative value indicating biomass during day higher than night. Note different scales on the y-axis among panels.

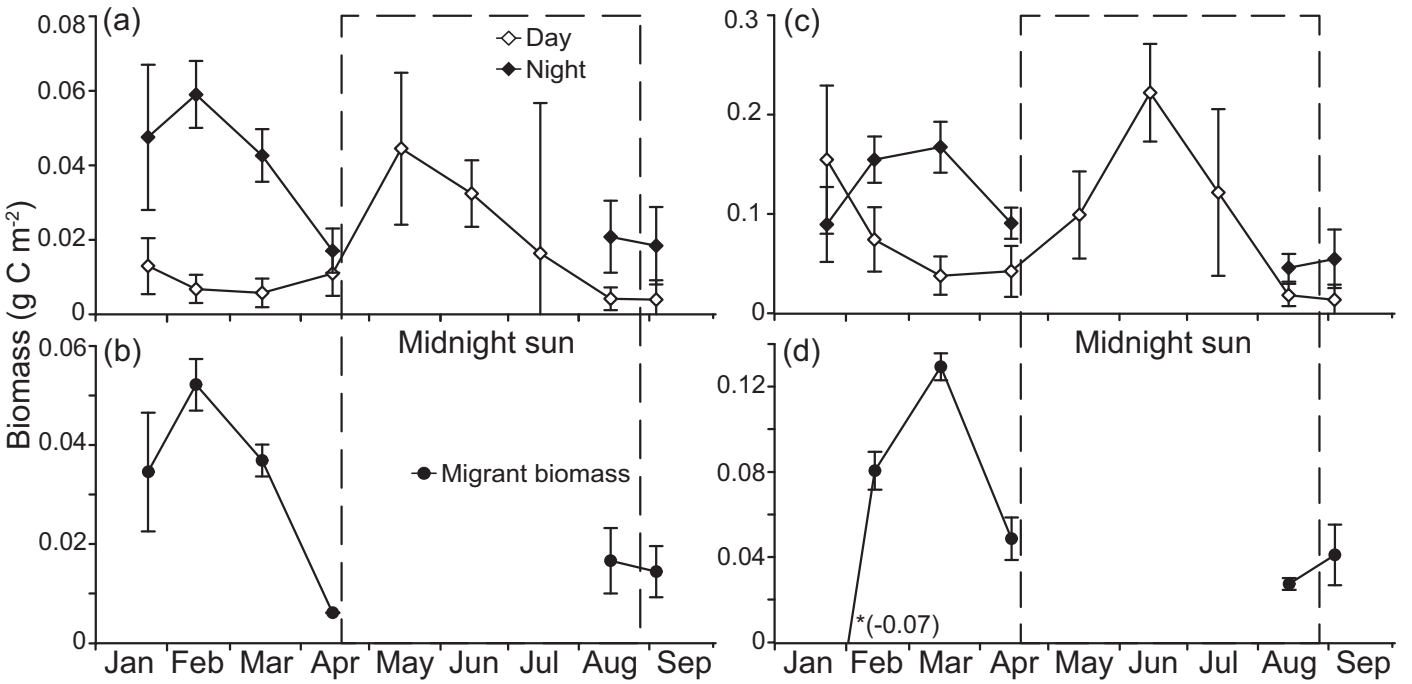


**Fig. 9.** Chaetognaths. (**a** and **c**) time series of average monthly day and night biomass (± 1 SE) in the 40 m and 82 m above the AZFP, respectively, and (**b** and **d**) respective diel migrant biomass (± 1 SE) in the same layers, with *negative value indicating biomass during day higher than night. Note different scales on the y-axis among panels.

deeper at day) was first measured in March with a maximum of 0.03 g $m^{-2}$ (Fig. 8b). The migrant biomass of chaetognaths showed a pattern similar to the one for euphausiids in the top 40 m and 82 m of the water column (Fig. 9b,d).

Averaged over the entire study period, the migrant biomass of euphausiids was about 34 and 6 times higher than the sum of copepod and chaetognath biomass in the top 40 m and 82 m layers, respectively.

**Respiration and excretion per unit mass**

Hourly rates of respiratory carbon loss per unit mass of the euphausiids *Thysanoessa* spp. in the uppermost 30 m varied little between January, May, and September (range 0.48–0.51 $\mu$g C mg $C^{-1}$ $h^{-1}$) (Table 2). The specific respiration of *Thysanoessa* spp. was in the same range as that of the other macrozooplankton taxa: *T. abyssorum* and *T. libellula*. Surprisingly, specific respiration of the two mesozooplankton size classes was high (> 2.5 $\mu$g C mg $C^{-1}$ $h^{-1}$) in January when food is supposed to be scarce. The respiration rate of the > 1000 $\mu$m fraction in January was significantly higher than in May and September (Kruskal-Wallis test; $p = 0.0157$). For the 200-$\mu$m to 1000-$\mu$m fraction, the respiration was only significantly higher in January than in September (Kruskal-Wallis test; $p = 0.0007$).

The euphausiid *Thysanoessa* spp. showed higher specific hourly rates of ammonium excretion around the September equinox ($0.06 \pm 0.03$ $\mu$g N mg $C^{-1}$ $h^{-1}$) than during the polar night ($0.03 \pm 0.01$ $\mu$g N mg $C^{-1}$ $h^{-1}$) (Kruskal-Wallis test; $p = 0.0058$). The specific excretion rate of the large and small mesozooplankton, however, did not differ between January and September, contrary to what was observed in the case of respiration. Pooling together the values of January and September yielded mean specific excretion rates of $0.97 \pm 0.89$ $\mu$g N mg $C^{-1}$ $h^{-1}$ and $0.62 \pm 0.27$ $\mu$g N mg $C^{-1}$ $h^{-1}$ for the large and small mesozooplankton, respectively.

**Community metabolism and active C and N transport**

For euphausiids, the mean of all measured specific respiration ($0.50 \pm 0.20$ $\mu$g C mg $C^{-1}$ $h^{-1}$) was used to calculate the community respiration in the top layers and the active respiratory transport of carbon (Eq. 5) below the targeted depths. For excretion rates, it was assumed that the low rate measured for euphausiids in January ($0.03 \pm 0.01$ $\mu$g N mg $C^{-1}$ $h^{-1}$) persisted until April, before the onset of primary production. The higher rate ($0.06 \pm 0.03$ $\mu$g N mg $C^{-1}$ $h^{-1}$) was then applied for the remaining of the study period to estimate community ammonium excretion and active transport of nitrogen. The reasons for the higher specific respiration rate of mesozooplankton in January compared to May and September are unknown, but most likely not due to strong feeding activity. This complicated the selection of logical cut-off points between January and May to discriminate periods when different specific respiration rates should be applied. Therefore, the specific respiration rates for January, May, and September were pooled to give a mean specific respiration rate of mesozooplankton of $1.75 \pm 1.06$ $\mu$g C mg

**Table 2.** Respiration and ammonium excretion rates per unit mass of zooplankton size classes and taxa in Kongsfjorden, Svalbard, Barents and Greenland Sea, and Bransfield Strait, Southern Ocean. Values are means ± 1 SD with number of measurements in parentheses.

| Taxon | Month | Temp. (°C) | Respiration ($\mu$g C mg $C^{-1}$ $h^{-1}$) | Excretion ($\mu$g N mg $C^{-1}$ $h^{-1}$) | Source |
|---|---|---|---|---|---|
| *Thysanoessa* spp. | Jan | 2.5 | 0.49 ± 0.21 (22) | 0.03 ± 0.01 (14) | 0 |
| | Apr | 4 | 0.58 ± 0.10 (8) | 0.07 ± 0.02 (8) | 6 |
| | May | 2.5 | 0.48 ± 0.09 (6) | – | 0 |
| | May | 0.1 | 0.76 ± 0.26 (11) | 0.02 ± 0.01 (11) | 4 |
| | May | 1.9 | 0.43 ± 0.12 (8) | 0.04 ± 0.01 (8) | 4 |
| | Aug | 4 | 0.58 ± 0.14 (8) | 0.06 ± 0.03 (8) | 6 |
| | Sep | 2.5 | 0.51 ± 0.21 (17) | 0.06 ± 0.03 (14) | 0 |
| Mesozooplankton | Jan | 2.5 | 2.66 ± 0.84 (6) | 0.78 ± 0.32 (6) | 0 |
| (>1000 $\mu$m) | May | 1–2.5 | 1.64 ± 0.21 (12) | – | 0 |
| | Sep | 2.5 | 1.56 ± 0.35 (15) | 1.09 ± 0.76 (9) | 0 |
| | Dec* | 0–2.3 | 2.45 ± 1.56 (20) | 0.38 ± 0.16 (20) | 1 |
| Mesozooplankton | Jan | 2.5 | 2.85 ± 0.39 (6) | 0.55 ± 0.11 (6) | 0 |
| (200–1000 $\mu$m) | May | 1–2.5 | 2.28 ± 0.5 (12) | – | 0 |
| | Sep | 2.5 | 1.72 ± 0.34 (15) | 0.67 ± 0.11 (9) | 0 |
| | Dec* | 0–2.3 | 2.27 ± 1.74 (3) | 0.17 ± 0.12 (3) | 1 |
| Mesozooplankton | Feb | −1.7 | 0.60 ± 0.24 (4) | – | 2 |
| (mixed; >200 $\mu$m) | May | −1.7 | 0,47 ± 0.12 (4) | – | 2 |
| | Jul | −1.3–6.6 | 0.81 ± 0.46 (19) | 0.22 ± 0.15 (19) | 3 |
| | Jul | 6.6 | 1.83 ± 0.19 (4) | 0.68 ± 0.31 (4) | 3 |
| | Sep | −1 | 0.55 ± 0.12 (3) | – | 2 |
| *P. elegans* | May | −0.3 | 0.40 ± 0.10 (12) | 0.15 ± 0.12 (12) | 4 |
| *T. abyssorum* | Jan | 2.5 | 1.08 ± 0.17 (8) | 0.26 ± 0.01 (5) | 0 |
| | Apr | 1–2.5 | 0.36 ± 0.11 (6) | – | 0 |
| | May | 1–2.5 | 0.50 ± 0.26 (3) | – | 0 |
| | Sep | 2.5 | 0.66 ± 0.10 (4) | 0.07 ± 0.01 (4) | 0 |
| *T. libellula* | Jan | 2.5 | 0.76 ± 0.14 (7) | 0.16 ± 0.03 (2) | 0 |
| | Apr | 1–2.5 | 0.18 ± 0.01 (3) | – | 0 |
| | May | 1–2.5 | 1.72 ± 0.28 (7) | – | 0 |
| | May | −0.1 | 0.92 ± 0.23 (11) | 0.03 ± 0.01 (11) | 4 |
| | Aug | 0 | 0.55 ± 0.18 (25) | – | 5 |
| | Sep | 2.5 | 0.39 ± 0.17 (8) | 0.02 ± 0.01 (3) | 0 |

(0) This study; (1) Hernández-León et al. (1999), * December corresponds to summer at the Antarctic peninsula; (2) Welch et al (1997); (3) Alcaraz et al. (2010), mean of all measurements, highest value measured during study; (4) Ikeda and Skjoldal (1989); (5) Auel and Werner (2003); (6) Huenerlage et al (2015).

$C^{-1}$ $h^{-1}$ that was used to calculate community daily respiration and active carbon flux due to DVM. Since there was no difference in ammonium excretion rate per unit mass measured in January and September, the mean specific excretion rates of 0.97 ± 0.89 $\mu$g N mg $C^{-1}$ $h^{-1}$ was applied in the equations.

Because of the high variability in the euphausiid biomass in the top layers, the monthly respiratory carbon loss of the euphausiid community was variable (Table 3). In the uppermost 40 m, community respiration remained above 4 mg C $m^{-2}$ $d^{-1}$ from January to March, at the height of winter DVM activity (Fig. 7). Daily respiration dropped in April when zooplankton spent only a few hours a day in the surface layer (Fig. 4), before recovering during the midnight sun period in May–June at the onset of the spring bloom period (Fig. 3). In the post-bloom conditions of July to early September, respiration reached again low levels compared to the winter and bloom periods. In the uppermost 82 m of the water column, euphausiid respiration showed a pattern similar to the one for the 2–40 m layer in winter and late summer. However, maximum respiration (> 38 mg C $m^{-2}$ $d^{-1}$) was reached in June when fluorescence at 37 m depth peaked.

Copepods showed less variability and seasonal fluctuation in their daily respiration than did euphausiids (Table 3).

**Table 3.** Monthly average (± 1 SD) of euphausiids, copepods and chaetognaths daily respiration in, and export of carbon from the 40 m and 82 m top layers in Kongsfjorden in 2014.

| | Respiration (mg C $m^{-2}$ $d^{-1}$) | | Respiratory transport (mg C $m^{-2}$ $d^{-1}$) | |
|---|---|---|---|---|
| **Month** | **2–40 m** | **2–82 m** | **Below 40 m** | **Below 82 m** |
| | Euphausiids | Euphausiids | Euphausiids | Euphausiids |
| Jan | 8.6 ± 7.2 | 19.1 ± 15.5 | 1.3 ± 1.0 | – |
| Feb | 7.7 ± 7.0 | 21.7 ± 23.2 | 3.5 ± 2.0 | 05.1 ± 2.6 |
| Mar | 4.1 ± 5.9 | 15.9 ± 23.4 | 4.6 ± 3.1 | 13.3 ± 5.9 |
| Apr | 1.8 ± 4.5 | 07.7 ± 24.6 | 1.0 ± 0.2 | 06.4 ± 9.3 |
| May | 7.1 ± 16.0 | 15.4 ± 35.6 | – | – |
| Jun | 5.8 ± 7.8 | 38.3 ± 46.7 | – | – |
| Jul | 2.6 ± 9.5 | 19.7 ± 36.7 | – | – |
| Aug | 1.1 ± 4.0 | 03.8 ± 13.0 | 2.4 ± 4.3 | 04.9 ± 5.7 |
| Sep | 1.2 ± 3.0 | 03.5 ± 09.1 | 2.1 ± 2.1 | 05.2 ± 4.3 |
| | Copepods | Copepods | Copepods | Copepods |
| Jan | 07.7 ± 3.1 | 15.9 ± 14.4 | – | – |
| Feb | 09.0 ± 3.4 | 20.0 ± 17.5 | – | 0.8 ± 3.2 |
| Mar | 08.8 ± 5.0 | 17.6 ± 15.9 | 0.9 ± 1.0 | 5.1 ± 6.8 |
| Apr | 09.7 ± 3.2 | 13.1 ± 09.9 | 1.0 ± 0.3 | 5.3 ± 8.2 |
| May | 10.5 ± 5.9 | 15.7 ± 16.8 | – | – |
| Jun | 13.8 ± 9.1 | 43.3 ± 43.0 | – | – |
| Jul | 13.3 ± 39.3 | 17.5 ± 12.8 | – | – |
| Aug | 09.0 ± 3.1 | 10.5 ± 05.1 | 0.3 ± 0.6 | 1.1 ± 6.2 |
| Sep | 08.3 ± 2.0 | 09.8 ± 04.0 | 0.3 ± 0.3 | 1.4 ± 7.2 |
| | Chaetognaths | Chaetognaths | Chaetognaths | Chaetognaths |
| Jan | 0.4 ± 0.3 | 1.0 ± 0.8 | 0.1 ± 0.0 | |
| Feb | 0.4 ± 0.4 | 1.2 ± 1.3 | 0.2 ± 0.1 | 0.3 ± 0.2 |
| Mar | 0.2 ± 0.3 | 0.8 ± 1.1 | 0.2 ± 0.1 | 0.7 ± 0.2 |
| Apr | 0.1 ± 0.3 | 0.4 ± 1.3 | <0.1 | 0.4 ± 0.4 |
| May | 0.4 ± 1.1 | 0.9 ± 2.3 | – | – |
| Jun | 0.3 ± 0.5 | 2.1 ± 2.6 | – | – |
| Jul | 0.2 ± 2.1 | 1.2 ± 4.4 | – | – |
| Aug | 0.1 ± 0.2 | 0.2 ± 0.6 | 0.1 ± 0.3 | 0.2 ± 0.1 |
| Sep | 0.1 ± 0.2 | 0.2 ± 0.5 | 0.1 ± 0.1 | 0.3 ± 0.3 |

**Table 4.** Monthly average (± 1 SD) of euphausiids, copepods and chaetognaths daily excretion in, and export of nitrogen from the 40 m and 82 m top layers in Kongsfjorden in 2014.

| | Excretion (mg N $m^{-2}$ $d^{-1}$) | | Excretory transport (mg N $m^{-2}$ $d^{-1}$) | |
|---|---|---|---|---|
| **Month** | **0–40 m** | **0–80 m** | **Below 40 m** | **Below 80 m** |
| | Euphausiids | Euphausiids | Euphausiids | Euphausiids |
| Jan | 0.53 ± 0.45 | 1.19 ± 0.96 | 0.08 ± 0.06 | – |
| Feb | 0.48 ± 0.43 | 1.35 ± 1.44 | 0.22 ± 0.13 | 0.32 ± 0.16 |
| Mar | 0.25 ± 0.37 | 0.99 ± 1.46 | 0.28 ± 0.19 | 0.83 ± 0.36 |
| Apr | 0.11 ± 0.28 | 0.48 ± 1.53 | 0.06 ± 0.01 | 0.40 ± 0.58 |
| May | 0.86 ± 1.94 | 1.87 ± 4.31 | – | – |
| Jun | 0.70 ± 0.94 | 4.63 ± 5.64 | – | – |
| Jul | 0.31 ± 1.15 | 2.39 ± 4.44 | – | – |
| Aug | 0.13 ± 0.48 | 0.46 ± 1.57 | 0.29 ± 0.52 | 0.60 ± 0.68 |
| Sep | 0.15 ± 0.37 | 0.43 ± 1.10 | 0.25 ± 0.25 | 0.63 ± 0.52 |
| | Copepods | Copepods | Copepods | Copepods |
| Jan | 4.28 ± 1.73 | 08.79 ± 8.00 | – | – |
| Feb | 4.99 ± 1.87 | 11.08 ± 9.72 | – | 0.43 ± 1.78 |
| Mar | 4.88 ± 2.75 | 09.73 ± 8.79 | 0.48 ± 0.53 | 2.83 ± 3.78 |
| Apr | 5.35 ± 1.76 | 07.24 ± 5.51 | 0.53 ± 0.16 | 2.93 ± 4.53 |
| May | 5.81 ± 3.26 | 08.71 ± 9.31 | – | – |
| Jun | 7.65 ± 5.07 | 23.97 ± 23.82 | – | – |
| Jul | 7.35 ± 21.77 | 09.68 ± 7.08 | – | – |
| Aug | 4.97 ± 1.73 | 05.82 ± 2.85 | 0.15 ± 0.34 | 0.61 ± 3.41 |
| Sep | 4.62 ± 1.12 | 05.45 ± 2.24 | 0.14 ± 0.18 | 0.78 ± 3.99 |
| | Chaetognaths | Chaetognaths | Chaetognaths | Chaetognaths |
| Jan | 0.15 ± 0.12 | 0.37 ± 0.32 | 0.02 ± 0.02 | – |
| Feb | 0.15 ± 0.14 | 0.45 ± 0.50 | 0.07 ± 0.03 | 0.10 ± 0.06 |
| Mar | 0.07 ± 0.10 | 0.32 ± 0.43 | 0.08 ± 0.04 | 0.28 ± 0.08 |
| Apr | 0.04 ± 0.12 | 0.16 ± 0.49 | 0.02 ± 0.00 | 0.15 ± 0.17 |
| May | 0.16 ± 0.41 | 0.36 ± 0.88 | – | – |
| Jun | 0.12 ± 0.18 | 0.80 ± 0.97 | – | – |
| Jul | 0.06 ± 0.81 | 0.44 ± 1.67 | – | – |
| Aug | 0.02 ± 0.07 | 0.07 ± 0.23 | 0.05 ± 0.12 | 0.09 ± 0.05 |
| Sep | 0.02 ± 0.06 | 0.07 ± 0.19 | 0.04 ± 0.05 | 0.12 ± 0.13 |

Throughout the study period, the community respiration ranged from 8–14 mg C $m^{-2}$ $d^{-1}$ and 10–43 mg C $m^{-2}$ $d^{-1}$ in the 2–40 m and 2–82 m layers, respectively, with the highest values in June. Overall, copepod community respiration was approximately 2 times higher than euphausiid respiration in the top 40 m while they were the same in the top 80 m of the water column. Chaetognath respiration was lower, being 43 and 19 times less than copepod and euphausiid respiration, respectively, in the top 40 m. The daily active respiratory transport of carbon due to copepod and chaetognath DVM peaked in March-April. Averaged over the study period, euphausiids exported 10 and 3 times more carbon during their DVM out of the top 40 m and 82 m layers, respectively, than copepods, and about 18 times more than chaetognaths for the two layers.

The highest estimates of euphausiid community excretion of ammonium were found during the main primary production season in May-June in the uppermost 40 m (> 0.7 mg N $m^{-2}$ $d^{-1}$) and June-July in the 2–82 layer (> 2 mg N $m^{-2}$ $d^{-1}$) (Table 4). During the winter months and the post-bloom period, the stable daily excretion ranged 0.1–0.5 mg N $m^{-2}$ $d^{-1}$ and 0.4–1.9 mg N $m^{-2}$ $d^{-1}$ in the two top layers. The DVM-mediated export of nitrogen out of the 40 m and 82 m top layers was lower at the end and right after the polar night (January-February), and at the start of the midnight sun prior to the spring bloom (April).

Copepod daily excretion of ammonium was about 14 and 6 times the euphausiid excretion in the 2–40 m and 2–82 m surface layers, respectively. Copepod excretion reached a maximum in June with a steep peak in the 2–82 m layer (24 mg N $m^{-2}$ $d^{-1}$). Active export of N due to copepod DVM culminated in March-April. On average, copepods transported 30% more N out of uppermost 40 m than euphausiids and 4 times more from the 2–82 m layer during the winter period. On the other hand, euphausiids exported 30% more and 6% less N than copepods did from the same two layers, respectively, during the post-bloom period. In comparison with euphausiids and copepods, chaetognaths had lower excretion rates that were never > 0.8 mg N $m^{-2}$ $d^{-1}$ in the two studied layers. Their capacity to transport N below these layers was thus low compared to the two other zooplankton groups.

## Sinking flux of POC and PON

Sinking POC flux integrated over the winter period 21 January–3 April was 0.7 g $m^{-2}$ at 40 m depth in 2014, and 2.1 g $m^{-2}$ at 100 m depth in 2013. Over the period 9 August–6 September, similar in duration to the autumn DVM period sampled in our study (11 August–9 September), the POC flux was 0.7 g $m^{-2}$ at 100 m depth in 2013.

In the same winter period as above, the sinking PON flux was 0.25 g $m^{-2}$ at 40 m depth in 2014, and 0.37 g $m^{-2}$ at 100 m depth in 2013. In the autumn period, the PON flux was 0.12 g $m^{-2}$ at 100 m depth in 2013.

## Discussion

### Seasonal variability in DVM

The visual analysis of the data from the moored AZFP multifrequency echosounder identified classical DVM from the end of January to mid-April, and recorded the onset of autumn DVM in mid-August (Fig. 3). Previous observations at the same site based on ADCP data collected from 2006 to 2008 suggest that the autumn DVM period lasted until mid-November (Wallace et al. 2010), which would make the two DVM phases equal in duration. During the DVM periods, zooplankton moved synchronously in and out of the uppermost layer of the water column over depth ranges of 40 m (depth of sediment traps) and 82 m (deepest threshold sampled by the AZFP) that are relevant for vertical fluxes of elements. Covering almost the entire water column, the ADCP echogram in late September showed DVM amplitudes of 120–140 m at the autumn equinox (Fig. 4). The two periods of classical synchronous DVM were out of phase with the period of high pelagic primary productivity, most probably reducing the contribution of active transport to the biological pump. Such uncoupling between DVM and the phytoplankton bloom was also observed in 2007 and 2008 in Kongsfjorden (Wallace et al. 2010), and this pattern is likely the rule rather than the exception in high-Arctic ecosystems. Here, there is generally a single bloom, usually between late April and August (Daase et al. 2013), and during a period of reduced diel light variation due to midnight sun. With the ongoing loss of Arctic sea ice, many regions at the periphery of the shrinking perennial ice pack are developing a second bloom in the autumn (Ardyna et al. 2014), and it is likely that this will coincide with the autumn DVM phase. Thus, we can expect classic DVM to have a growing role in the biological pump if these observed changes in phytoplankton seasonality amplify in the future.

Combining the AZFP data analysis with morphometric information on zooplankton caught in nets allowed us to identify euphausiids as the major diel migrants in terms of biomass in the fjord in 2014. This finding was further validated with plankton net data limited to January and September that showed that euphausiids of the genus *Thysanoessa* made up the bulk of macrozooplankton biomass (> 90%) at night. We also attributed the high backscatter in the surface layer in June to the presence of *Thysanoessa* spp., although macrozooplankton were not sampled quantitatively with nets during the spring-summer season due to the unavailability of a ship large enough for trawling large plankton nets. Temperature profiles above 2°C throughout the water column in May and July revealed no significant intrusion of cold Arctic Water into Kongsfjorden. Furthermore, mesozooplankton data from the same period indicate no change in the community that could have signaled a massive advection of Arctic zooplankton. Thus, we assumed that the macrozooplankton size class, dominated by the arcto-boreal *Thysanoessa* spp. during winter, did not shift either to a more Arctic assemblage during the period of high biological production. It is possible, however, that larger macrozooplankton like the more Atlantic *Meganyctiphanes norvegica* were underestimated in the net samples as they could possibly avoid the net type and trawl short duration used.

Large copepods (dominated by *Calanus* spp.) and chaetognaths (essentially *P. elegans*) also performed diel migrations during the two DVM periods. Nevertheless, zooplankton biomass derived from the calibrated AZFP revealed that euphausiids generally contributed > 90% of the total diel migrant biomass (euphausiids + copepods + chaetognaths) in the uppermost 40 m and 82 m. The unverified assumption of a monospecific zooplankton assemblage in each echo-integration cell of the acoustic analysis may have had an effect on the estimation of biomass that is difficult to evaluate. However, we are confident that the small size selected for the cells (1-m vertical by 5-min horizontal) tempers this effect. The daily zooplankton migrant biomass below 82 m during the transition from polar night to midnight sun and in late summer in Kongsfjorden exceeded most of the estimates for other systems where active fluxes due to DVM were studied (Supporting Information Table S3). Our range of estimates did encompass the higher values measured off the Canary Islands and in the North Pacific (Yebra et al.

2005; Steinberg et al. 2008; Takahashi et al. 2009). One of the plausible reasons for the discrepancy between our high estimates and those of other studies is that most of these others did not include the macrozooplankton size class, which dominated zooplankton migrant biomass in Kongsfjorden. Therefore, their assessment of the importance of zooplankton active fluxes of carbon and nitrogen may well be very conservative.

**Zooplankton metabolism**

This study significantly expands on the limited knowledge of respiration and ammonium excretion rates of arctic euphausiids. The mass-specific respiration rates of *Thysanoessa* spp. (mainly *T. inermis*) in winter, spring and autumn 2014 were close to the value found in April (pre-bloom period) and August (post-bloom) for *T. inermis* in Kongsfjorden (Huenerlage et al. 2015), and within the range of values in late May in the eastern Barents Sea (Ikeda and Skjoldal 1989). We did not observe a lower specific respiration during the polar night period of food scarcity compared to the pre-bloom period or to the autumn equinox, supporting the suggestion of Huenerlage et al. (2015) that *Thysanoessa* spp. do not reduce their metabolism in winter. It is possible that respiration rates were higher during the bloom period, between late May and June, when the mainly herbivore *T. inermis* ingests large quantities of pelagic algae to build its lipid reserves. If so, our estimates of euphausiid community respiration for the summer period would be conservative. Mass-specific ammonium-excretion rates of *Thysanoessa* spp. in our study are consistent with those measured by Ikeda and Skjoldal (1989) and Huenerlage et al. (2015). The lower excretion rate in January than in September is presumably due to better feeding conditions in autumn, as excretion and ingestion rates are closely linked (Saborowski et al. 2002).

Overall, mesozooplankton respiration rates reported here are consistent with measurements on the same size classes during the Antarctic summer (Hernández-León et al. 1999), and the highest value measured on total mesozooplankton (not size-fractionated) from north-Svalbard in summer (Alcaraz et al. 2010). But we measured higher mass-specific respiration rates than Welch et al. (1997) did in the colder waters of the Canadian Arctic archipelago. Likewise, mesozooplankton ammonium excretion rates in Kongsfjorden were 1–3.5 times higher than the rates for Antarctica and north-Svalbard (Table 2).

Pelagic primary production estimates in Kongsfjorden are scarce and not available for 2014. Hodal et al. (2012) calculated a gross primary production (GPP) of 27–35 g C $m^{-2}$ in the 0–40 m layer during the spring bloom of 2002 (18 April–13 May), consistent with previous annual GPP estimates of 25–30 g C $m^{-2}$ in the northeast Barents Sea (Hegseth 1998). Thus, assuming the same range of GPP in 2014 as in 2002, euphausiids would have used 0.7–0.9% and large copepods 1.3–1.7% of the phytoplankton carbon produced to cover their respiratory carbon loss (Rc) during the bloom, here circumscribed to 15 May–20 June. These fractions are much less than the 5–67% (average 23%) of GPP that mesozooplankton respiration alone accounted for in the northwest Barents Sea (Alcaraz et al. 2010). However, it is important to bear in mind that our metabolic measurements were not made during bloom conditions and, thus, are likely underestimates of respiration and excretion during the bloom period. A rough estimate of zooplankton ingestion (I), using the equation of Ikeda and Motoda (1978) in which $I = 2.5$ Rc, shows that combined euphausiid-copepod grazing would account for 5–6% of GPP, a range below the 22–44% of GPP intercepted by zooplankton in the northeast Barents Sea (Wexels Riser et al. 2008), or 45% by copepods in the Greenland Northeast Water Polynya (Daly 1997). Using the Redfield ratio to convert phytoplankton carbon production to nitrogen production, euphausiid and mesozooplankton $NH4^+$ excretion in the uppermost 40 m would support 5–7% of the bloom GPP. This is again low compared to the 9–242% (mean 59%) that mesozooplankton alone re-supplied in the photic layer of the northern Barents Sea for phytoplankton production in July (Alcaraz et al. 2010). Therefore, we suggest that the effect of zooplankton grazing and excretion on phytoplankton total production was weak in Kongsfjorden during the bloom of 2014.

**Active export of dissolved carbon and nitrogen mediated by DVM**

The active transport of carbon due to synchronous migration by euphausiids, large copepods and chaetognaths was 0.3 g $m^{-2}$ and 0.9 g $m^{-2}$ below 40 m and 82 m depth, respectively, during the 2014 winter DVM period in Kongsfjorden (31 January–11 April), and 0.2 g $m^{-2}$ below 82 m at the onset of the autumn DVM (from 11 August to 9 September). Thus, the DVM-mediated carbon transport would represent $>40\%$ of the winter carbon sinking flux of POC measured in sediment traps, and $>25\%$ of the sinking flux during the first weeks of autumn. These ratios of active to passive carbon export fall within the range of ratios for daily fluxes (13–70%) in several oligotrophic and more seasonally stable sub-Arctic to equatorial systems (Dam et al. 1995; Zhang and Dam 1997; Hernández-León et al. 2001; Yebra et al. 2005; Stukel et al. 2013) (Supporting Information Table S3). Representing $>25\%$ of POC sinking flux, the DVM transport in Kongsfjorden was higher than other estimates (1–14% of sinking flux) for different times of the year in the subtropical Atlantic, Bermuda, around the Canary Islands, and from equatorial to subarctic Pacific regions (Le Borgne and Rodier 1997; Rodier and Le Borgne 1997; Kobari et al. 2008; Putzeys et al. 2011). The 0.9 g C $m^{-2}$ transported by winter DVM in Kongsfjorden represents 30% of the active flux by *Calanus* spp. (mainly *C. hyperboreus*) SVM below 100 m (3.1 g C $m^{-2}$) during the overwintering period (October–April) in the southeastern Beaufort Sea (Darnis and

Fortier 2012). Adding the amount transported to depth by autumn DVM could possibly double the contribution of DVM-mediated transport over an annual cycle. Using short-term sediment trap deployments (21–52 h) in Kongsfjorden in 2012–2013, Lalande et al. (2016) provide three estimates of daily sinking POC fluxes: during a bloom in May, and post-bloom conditions in August and October (Supporting Information Table S5). Comparison between daily active transport below 82 m and the mean post-bloom POC flux in 2012 ($167 \pm 88$ mg C $m^{-2}$ $d^{-1}$ at 100 m) yields active to passive export ratios from 4–12% that are within the range of low ratios published. To estimate the active transports, the zooplankton groups were assumed not to feed at depth. This may have been the case for copepods and euphausiids but not for the carnivorous chaetognaths. However, the latter represented a minor fraction of the migrant biomass. Although not ideal, such comparisons involving different years, locations, and seasons reveal all the same that, despite the complex DVM regime at high latitudes, the active carbon transport due to DVM in Kongsfjorden is close to what has been reported in lower latitude regions of the World Ocean.

Zooplankton winter DVM transported 0.03 g N $m^{-2}$ and 0.18 g N $m^{-2}$ out of the 40 m and 82 m top water layers, respectively, whereas early autumn DVM transported 0.04 g N $m^{-2}$ out the 100 m top layer. The DVM-mediated active transport of nitrogen represents thus 12% and 49% of the PON sinking flux at 40 m and 100 m integrated over the winter period, and 33% of the sinking flux at 100 m in early autumn. Such ratios of active to passive export of nitrogen fall well within the wide range of ratios (7–108% of daily PON flux) stemming from the few studies addressing active transport of nitrogen due to DVM (Longhurst and Harrison 1988; Longhurst et al. 1989; Al-Mutairi and Landry 2001; Steinberg et al. 2002) (Supporting Information Table S4). On a daily basis, however, estimates of active N transport due to euphausiid, copepod, and chaetognath represent 4–18% of the mean sinking flux of PON ($21 \pm 7$ mg N $m^{-2}$ $d^{-1}$) below 100 m during the post-bloom conditions in 2012 (Supporting Information Table S5). Our daily ratios thus lie at the lower range of published ratios. Interestingly, winter DVM and excretion at depth by large copepods contributed 76% of the active N transport, whereas it was euphausiid DVM and their respiration at depth that dominated in similar proportion (70%) the active C transport during the same period.

By using acoustic data with measurements of respiration and ammonium excretion, we have been able to describe for the first time the role of zooplankton DVM in the functioning of the biological pump of a high-latitude marine ecosystem. As expected, the active transport of carbon and nitrogen to depth through synchronous DVM is discontinuous over an annual cycle, due to the suspension of DVM during parts of the polar night and midnight sun (Cottier et al. 2006; Berge et al. 2009; Last et al. 2016). The fact that this process occurs essentially outside of the short season of high photosynthesis likely limits its function in the biological pump of Arctic ecosystems if an annual budget is to be estimated. On the other hand, this study also revealed that the importance of active transport in the Kongsfjorden ecosystem during times of strong DVM (winter and autumn) compared well with other oceanic systems. Since the winter DVM took place in a fully mixed water column in Kongsfjorden, the active transports estimated for winter cannot be regarded as export fluxes. But at other times of the year (Loeng 1991) and in other locations in the Arctic, DVM coincides with highly stratified water columns. Production of sinking fecal pellets, active transport of feces in the migrants' guts, high winter mortality at depth, and shedding of exuviae, should also be quantified and included in C and N budgets along with DVM-mediated flux of dissolved components measured here. If we are to achieve a realistic description of the biological pump of the Arctic marine ecosystems, it will be especially important to estimate these rates during the understudied periods outside of the short spring-summer season. Based on our results, it remains that respiratory C and excretory N transport due to DVM should be considered for flux estimation in the extensive Arctic regions permanently subject to haline stratification. Under the effect of global warming, the increased river runoff and sea ice melt will result in a better match in timing between DVM-mediated processes and stratification of the water column (Pemberton and Nilsson 2016), which should increase the efficiency of the biological carbon pump. Furthermore, Cottier et al. (2006) and Wallace et al. (2010) found evidence for unsynchronized migration in Kongsfjorden during the midnight sun in June. Zooplankton would swim individually in the surface layer, possibly to feed, and sink out during digestion repeatedly over a 24-h period. In 2014, June coincided with maximum fluorescence and zooplankton biomass in the 82 m surface layer. Direct vertical shunting of carbon and nitrogen to deeper less retentive layers due to this foray-type migration would enhance the efficiency of the biological pump when biological productivity is at its highest. However, unsynchronized migration needs to be investigated in other high-latitude regions. For instance, no unsynchronized migrations were detected during the midnight sun in the Antarctic Weddell Sea (Cisewski and Strass 2016) and over the West Spitsbergen outer shelf (Geoffroy et al. 2016).

The finding of the prominent role of euphausiids (particularly *Thysanoessa* spp.) in the active vertical transport of carbon has also been reported lately in the North-west Mediterranean Sea (Isla et al. 2015). Euphausiids are abundant in the shelf seas on the Pacific side of the Arctic as well (Eisner et al. 2013) where there is a stronger stratification of the water column. Over the Arctic continental slopes and basins, little is known about the distribution of macrozooplankton and it is assumed so far that long-range SVM by large *C. hyperboreus* is the main pathway for the active

vertical flux of carbon (Hirche 1997; Darnis and Fortier 2012). To be able to fully assess the function of zooplankton migrations in the biological pump on a pan-Arctic scale, we need to define better the biogeography, feeding biology, and migratory parameters (depth range, swimming speed, time at depth) of key zooplankton taxa, namely the Arctic *Calanus* spp., the arcto-boreal *Thysanoessa* spp. and other macrozooplankton like *Themisto* spp.

## References


Alcaraz, M., and others. 2010. The role of arctic zooplankton in biogeochemical cycles: Respiration and excretion of ammonia and phosphate during summer. Polar Biol. **33**: 1719–1731. doi:10.1007/s00300-010-0789-9

Al-Mutairi, H., and M. R. Landry. 2001. Active export of carbon and nitrogen at Station ALOHA by diel migrant zooplankton. Deep-Sea Res. Part II **48**: 2083–2103. doi:10.1016/S0967-0645(00)00174-0

Ardyna, M., M. Babin, M. Gosselin, E. Devred, L. Rainville, and J. Tremblay. 2014. Recent Arctic Ocean sea ice loss triggers novel fall phytoplankton blooms. Geophys. Res. Lett. **41**: 6207–6212. doi:10.1002/2014GL061047

ASL. 2014. AZFP (Acoustic Zooplankton Fish Profiler) operators manual, p. 77. ASL.

Auel, H., and I. Werner. 2003. Feeding, respiration and life history of the hyperiid amphipod *Themisto libellula* in the Arctic marginal ice zone of the Greenland Sea.. J. Exp. Mar. Biol. Ecol. **296**: 183–197.

Basedow, S. L., K. Eiane, V. Tverberg, and M. Spindler. 2004. Advection of zooplankton in an Arctic fjord (Kongsfjorden, Svalbard). Estuar. Coast. Shelf Sci. **60**: 113–124. doi:10.1016/j.ecss.2003.12.004

Benfield, M. C., C. S. Davis, and S. M. Gallager. 2000. Estimating the in-situ orientation of *Calanus finmarchicus* on Georges Bank using the Video Plankton Recorder. Plankton Biol. Ecol. **47**: 69–72.

Berge, J., and others. 2009. Diel vertical migration of Arctic zooplankton during the polar night. Biol. Lett. **5**: 69–72. doi:10.1098/rsbl.2008.0484

Berge, J., and others. 2014. Arctic complexity: A case study on diel vertical migration of zooplankton. J. Plankton Res. **36**: 1279–1297. doi:10.1093/plankt/fbu059

Berge, J., and others. 2015. In the dark: A review of ecosystem processes during the Arctic polar night. Prog. Oceanogr. **139**: 258–271. doi:10.1016/j.pocean.2015.08.005

Brierley, A. S. 2014. Diel vertical migration. Curr. Biol. **24**: R1074–R1076. doi:10.1016/j.cub.2014.08.054

Bronk, D. A., and D. K. Steinberg. 2008. Chapter 8 - nitrogen regeneration, p. 385–467. *In* D. G. Capone, D. A. Bronk, M. R. Mulholland, and E. J. Carpenter [eds.], Nitrogen in the marine environment, 2nd ed. Academic Press.

Chu, D., K. G. Foote, and T. K. Stanton. 1993. Further analysis of target strength measurements of Antarctic krill at 38 and 120 kHz: Comparison with deformed cylinder model and inference of orientation distribution. J. Acoust. Soc. Am. **93**: 2985–2988. doi:10.1121/1.405818

Cisewski, B., and V. H. Strass. 2016. Acoustic insights into the zooplankton dynamics of the eastern Weddell Sea. Prog. Oceanogr. **144**: 62–92. doi:10.1016/j.pocean.2016.03.005

Cottier, F., V. Tverberg, M. Inall, H. Svendsen, F. Nilsen, and C. Griffiths. 2005. Water mass modification in an Arctic fjord through cross-shelf exchange: The seasonal hydrography of Kongsfjorden, Svalbard. J. Geophys. Res. **110**: C12005. doi:10.1029/2004JC002757

Cottier, F. R., G. A. Tarling, A. Wold, and S. Falk-Petersen. 2006. Unsynchronized and synchronized vertical migration of zooplankton in a high Arctic fjord. Limnol. Oceanogr. **51**: 2586–2599. doi:10.4319/lo.2006.51.6.2586

Cottier, F. R., F. Nilsen, M. E. Inall, S. Gerland, V. Tverberg, and H. Svendsen. 2007. Wintertime warming of an Arctic shelf in response to large-scale atmospheric circulation. Geophys. Res. Lett. **34**: L10607. doi:10.1029/2007GL029948

Cottier, F. R., F. Nilsen, R. Skogseth, V. Tverberg, J. Skarðhamar, and H. Svendsen. 2010. Arctic fjords: A review of the oceanographic environment and dominant physical processes. Geol. Soc. London Spec. Publ. **344**: 35–50. doi:10.1144/SP344.4

Daase, M., K. Eiane, D. L. Aksnes, and D. Vogedes. 2008. Vertical distribution of *Calanus* spp. and *Metridia longa* at four Arctic locations. Mar. Biol. Res. **4**: 193–207. doi:10.1080/17451000801907948

Daase, M., and others. 2013. Timing of reproductive events in the marine copepod *Calanus glacialis*: A pan-Arctic perspective. Can. J. Fish. Aquat. Sci. **70**: 871–884. doi:10.1139/cjfas-2012-0401

Daly, K. L. 1997. Flux of particulate matter through copepods in the Northeast water polynya. J. Mar. Syst. **10**: 319–342. doi:10.1016/S0924-7963(96)00062-0

Dam, H. G., M. R. Roman, and M. J. Youngbluth. 1995. Downward export of respiratory carbon and dissolved inorganic nitrogen by diel-migrant mesozooplankton at the JGOFS Bermuda time-series station. Deep-Sea Res. Part I **42**: 1187–1197. doi:10.1016/0967-0637(95)00048-B

Darnis, G., and L. Fortier. 2012. Zooplankton respiration and the export of carbon at depth in the Amundsen Gulf (Arctic Ocean). J. Geophys. Res. **117**: C04013. doi:10.1029/2011JC007374

Ducklow, H. W., D. K. Steinberg, and K. O. Buesseler. 2001. Upper ocean carbon export and the biological pump. Oceanography **14**: 50–58. doi:10.5670/oceanog.2001.06

Eisner, L., N. Hillgruber, E. Martinson, and J. Maselko. 2013. Pelagic fish and zooplankton species assemblages in relation to water mass characteristics in the northern Bering and southeast Chukchi seas. Polar Biol. **36**: 87–113. doi:10.1007/s00300-012-1241-0

Fischer, J., and M. Visbeck. 1993. Seasonal variation of the daily zooplankton migration in the Greenland Sea. Deep-Sea Res. Part I Oceanogr. Res. Pap. **40**: 1547–1557. doi:10.1016/0967-0637(93)90015-U

Fortier, M., L. Fortier, H. Hattori, H. Saito, and L. Legendre. 2001. Visual predators and the diel vertical migration of copepods under Arctic sea ice during the midnight sun. J. Plankton Res. **23**: 1263–1278. doi:10.1093/plankt/23.11.1263

Geoffroy, M., F. R. Cottier, J. Berge, and M. E. Inall. 2016. AUV-based acoustic observations of the distribution and patchiness of pelagic scattering layers during midnight sun. ICES J. Mar. Sci. (Special issue 6th Zooplankton Production Symposium) doi:10.1093/icesjms/fsw158.

Gnaiger, E. 1983. Calculation of energetic and biochemical equivalents of respiratory oxygen consumption, p. 337–345. In E. Gnaiger and H. Forstner [eds.], Polarographic oxygen sensors: Aquatic and physiological applications. Springer-Verlag.

Hegseth, E. N. 1998. Primary production of the northern Barents Sea. Polar Res. **17**: 113–123. doi:10.1111/j.1751-8369.1998.tb00266.x

Hegseth, E. N., and V. Tverberg. 2013. Effect of Atlantic water inflow on timing of the phytoplankton spring bloom in a high Arctic fjord (Kongsfjorden, Svalbard). J. Mar. Syst. **113**: 94–105. doi:10.1016/j.jmarsys.2013.01.003

Hernández-León, S., S. Torres, M. Gomez, I. Montero, and C. Almeida. 1999. Biomass and metabolism of zooplankton in the Bransfield Strait (Antarctic Peninsula) during austral spring. Polar Biol. **21**: 214–219. doi:10.1007/s003000050355

Hernández-León, S., M. Gomez, M. Pagazaurtundua, A. Portillo-Hahnefeld, I. Montero, and C. Almeida. 2001. Vertical distribution of zooplankton in Canary Island waters: Implications for export flux. Deep-Sea Res. Part I **48**: 1071–1092. doi:10.1016/S0967-0637(00)00074-1

Hirche, H. J. 1997. Life cycle of the copepod *Calanus hyperboreus* in the Greenland Sea. Mar. Biol. **128**: 607–618. doi:10.1007/s002270050127

Hodal, H., S. Falk-Petersen, H. Hop, S. Kristiansen, and M. Reigstad. 2012. Spring bloom dynamics in Kongsfjorden, Svalbard: Nutrients, phytoplankton, protozoans and primary production. Polar Biol. **35**: 191–203. doi:10.1007/s00300-011-1053-7

Huenerlage, K., M. Graeve, C. Buchholz, and F. Buchholz. 2015. The other krill: Overwintering physiology of adult *Thysanoessa inermis* (Euphausiacea) from the high-Arctic Kongsfjord. Aquat. Biol. **23**: 225–235. doi:10.3354/ab00622

Ikeda, T., and S. Motoda. 1978. Estimated zooplankton production and their ammonia excretion in Kuroshio and adjacent seas. Fish. Bull. **76**: 357–367.

Ikeda, T., and H. R. Skjoldal. 1989. Metabolism and elemental composition of zooplankton from the Barents Sea during early Arctic summer. Mar. Biol. **100**: 173–183. doi:10.1007/BF00391956

Ingvarsdóttir, A., D. F. Houlihan, M. R. Heath, and S. J. Hay. 1999. Seasonal changes in respiration rates of copepodite stage V *Calanus finmarchicus* (Gunnerus). Fish. Oceanogr. **8**: 73–83. doi:10.1046/j.1365-2419.1999.00002.x

Isla, A., R. Scharek, and M. Latasa. 2015. Zooplankton diel vertical migration and contribution to deep active carbon flux in the NW Mediterranean. J. Mar. Syst. **143**: 86–97. doi:10.1016/j.jmarsys.2014.10.017

Kobari, T., D. K. Steinberg, A. Ueda, A. Tsuda, M. W. Silver, and M. Kitamura. 2008. Impacts of ontogenetically migrating copepods on downward carbon flux in the western subarctic Pacific Ocean. Deep-Sea Res. Part II Top. Stud. Oceanogr. **55**: 1648–1660. doi:10.1016/j.dsr2.2008.04.016

Kristensen, Å., and J. Dalen. 1986. Acoustic estimation of size distribution and abundance of zooplankton. J. Acoust. Soc. Am. **80**: 601–611. doi:10.1121/1.394055

Kwasniewski, S., H. Hop, S. Falk-Petersen, and G. Pedersen. 2003. Distribution of Calanus species in Kongsfjorden, a glacial fjord in Svalbard. J. Plankton Res. **25**: 1–20. doi:10.1093/plankt/25.1.1

Lalande, C., B. Moriceau, A. Leynaert, and N. Morata. 2016. Spatial and temporal variability in export fluxes of biogenic matter in Kongsfjorden. Polar Biol. **10**: 1725–1738. doi:1007/s00300-016-1903-4

Last, K. S., L. Hobbs, J. Berge, A. S. Brierley, and F. Cottier. 2016. Moonlight drives ocean-scale mass vertical migration of zooplankton during the Arctic winter. Curr. Biol. **26**: 1–8. doi:10.1016/j.cub.2015.11.038

Lawson, G. L., P. H. Wiebe, C. J. Ashjian, S. M. Gallager, C. S. Davis, and J. D. Warren. 2004. Acoustically-inferred zooplankton distribution in relation to hydrography west of the Antarctic Peninsula. Deep-Sea Res. Part II **51**: 2041–2072. doi:10.1016/j.dsr2.2004.07.022

Le Borgne, R., and M. Rodier. 1997. Net zooplankton and the biological pump: A comparison between the oligotrophic and mesotrophic equatorial Pacific. Deep-Sea Res. Part II **44**: 2003–2023. doi:10.1016/S0967-0645(97)00034-9

Loeng, H. 1991. Features of the oceanographic conditions of the Barents Sea, p. 5–18. *In* E. Sakshaug, C. C. E. Hopkins, and N. A. Øritsland [eds.], Proceedings of the Pro Mare Symposium on Polar Marine Ecology, Trondheim, 12–16 May 1990. Polar Research **10** (1).

Longhurst, A. R., and W. G. Harrison. 1988. Vertical nitrogen flux from the oceanic photic zone by diel migrant zooplankton and nekton. Deep-Sea Res. Part A **35**: 881–889. doi:10.1016/0198-0149(88)90065-9

Longhurst, A. R., A. Bedo, W. G. Harrison, E. J. H. Head, E. P. Horne, B. Irwin, and C. Morales. 1989. NFLUX-a test of vertical nitrogen flux by diel migrant biota. Deep-Sea Res. Part A **36**: 1705–1719. doi:10.1016/0198-0149(89)90067-8

Longhurst, A. R., A. W. Bedo, W. G. Harrison, E. J. H. Head, and D. D. Sameoto. 1990. Vertical flux of respiratory carbon by oceanic diel migrant biota. Deep-Sea Res. Part I **37**: 685–694. doi:10.1016/0198-0149(90)90098-G

Marinov, I., and J. L. Sarmiento. 2004. The role of the oceans in the global carbon cycle: An overview, p. 395. In M. Follows and T. Oguz [eds.], The ocean carbon cycle and climate. Kluwer Academic Publishers.

Parker-Stetter, S. L., L. G. Rudstam, P. J. Sullivan, and D. M. Warner. 2009. Standard operating procedures for fisheries acoustic surveys in the Great Lakes. p. 180. Great Lakes Fisheries Commission Special Publications 09–01.

Pemberton, P., and J. Nilsson. 2016. The response of the central Arctic Ocean stratification to freshwater perturbations. J. Geophys. Res. Oceans **121**: 792–817. doi:10.1002/2015JC011003

Putzeys, S., L. Yebra, C. Almeida, P. Becognee, and S. Hernandez-Leon. 2011. Influence of the late winter bloom on migrant zooplankton metabolism and its implications on export fluxes. J. Mar. Syst. **88**: 553–562. doi:10.1016/j.jmarsys.2011.07.005

Ringelberg, J. 2010. Diel vertical migration of zooplankton in lakes and oceans. Causal explanations and adaptive significances. Springer.

Rodier, M., and R. Le Borgne. 1997. Export flux of particles at the equator in the western and central Pacific ocean. Deep-Sea Res. Part II Top. Stud. Oceanogr. **44**: 2085–2113. doi:10.1016/S0967-0645(97)00092-1

Saborowski, R., S. Brohl, G. A. Tarling, and F. Buchholz. 2002. Metabolic properties of Northern krill, *Meganyctiphanes norvegica*, from different climatic zones. I. Respiration and excretion. Mar. Biol. **140**: 547–556. doi:10.1007/s00227-001-0730-4

Seuthe, L., K. R. Iversen, and F. Narcy. 2011. Microbial processes in a high-latitude fjord (Kongsfjorden, Svalbard): II. Ciliates and dinoflagellates. Polar Biol. **34**: 751–766. doi:10.1007/s00300-010-0930-9

Solórzano, L. 1969. Determination of ammonia in natural waters by the phenolhypochlorite method. Limnol. Oceanogr. **14**: 799–801. doi:10.4319/lo.1969.14.5.0799

Stanton, T. K., P. H. Wiebe, D. Chu, M. C. Benfield, L. Scanlon, L. Martin, and R. L. Eastwood. 1994. On acoustic estimates of zooplankton biomass. ICES J. Mar. Sci. **51**: 505–512. doi:10.1006/jmsc.1994.1051

Stanton, T. K., D. Chu, and P. H. Wiebe. 1998. Sound scattering by several zooplankton groups. II. Scattering models. J. Acoust. Soc. Am. **103**: 236–253. doi:10.1121/1.421110

Stanton, T. K., and D. Chu. 2000. Review and recommendations for the modelling of acoustic scattering by fluid-like elongated zooplankton: Euphausiids and copepods. ICES J. Mar. Sci. **57**: 793–807. doi:10.1006/jmsc.1999.0517

Steinberg, D. K., C. A. Carlson, N. R. Bates, S. A. Goldthwait, L. P. Madin, and A. F. Michaels. 2000. Zooplankton vertical migration and the active transport of dissolved organic and inorganic carbon in the Sargasso Sea. Deep-Sea Res. Part I **47**: 137–158. doi:10.1016/S0967-0637(99)00052-7

Steinberg, D. K., S. A. Goldthwait, and D. A. Hansell. 2002. Zooplankton vertical migration and the active transport of dissolved organic and inorganic nitrogen in the Sargasso Sea. Deep-Sea Res. Part I Oceanogr. Res. Pap. **49**: 1445–1461. doi:10.1016/S0967-0637(02)00037-7

Steinberg, D. K., B. A. S. Van Mooy, K. O. Buesseler, P. W. Boyd, T. Kobari, and D. M. Karl. 2008. Bacterial vs. zooplankton control of sinking particle flux in the ocean's twilight zone. Limnol. Oceanogr. **53**: 1327–1338. doi:10.4319/lo.2008.53.4.1327

Stukel, M. R., M. D. Ohman, C. R. Benitez-Nelson, and M. R. Landry. 2013. Contributions of mesozooplankton to vertical carbon export in a coastal upwelling system. Mar. Ecol. Prog. Ser. **491**: 47–65. doi:10.3354/meps10453

Svendsen, H., and others. 2002. The physical environment of Kongsfjorden-Krossfjorden, an Arctic fjord system in Svalbard. Polar Res. **21**: 133–166. doi:10.1111/j.1751-8369.2002.tb00072.x

Takahashi, K., A. Kuwata, H. Sugisaki, K. Uchikawa, and H. Saito. 2009. Downward carbon transport by diel vertical migration of the copepods *Metridia pacifica* and *Metridia okhotensis* in the Oyashio region of the western subarctic Pacific Ocean. Deep-Sea Res. Part I **56**: 1777–1791. doi:10.1016/j.dsr.2009.05.006

Wallace, M. I., F. R. Cottier, J. Berge, G. A. Tarling, C. Griffiths, and A. S. Brierley. 2010. Comparison of zooplankton vertical migration in an ice-free and a seasonally ice-covered Arctic fjord: An insight into the influence of sea ice cover on zooplankton behavior. Limnol. Oceanogr. **55**: 831–845. doi:10.4319/lo.2010.55.2.0831

Welch, H. E., T. D. Siferd, and P. Bruecker. 1996. Population densities, growth, and respiration of the chaetognath *Parasagitta elegans* in the Canadian high Arctic. Can. J. Fish. Aquat. Sci. **53**: 520–527. doi:10.1139/cjfas-53-3-520

Welch, H. E., T. D. Siferd, and P. Bruecker. 1997. Marine zooplanktonic and benthic community respiration rates at Resolute, Canadian high Arctic. Can. J. Fish. Aquat. Sci. **54**: 995–1005. doi:10.1139/f97-006

Wexels Riser, C., P. Wassmann, M. Reigstad, and L. Seuthe. 2008. Vertical flux regulation by zooplankton in the northern Barents Sea during Arctic spring. Deep-Sea Res. Part II **55**: 2320–2329. doi:10.1016/j.dsr2.2008.05.006

Willis, K., F. Cottier, S. Kwasniewski, A. Wold, and S. Falk-Petersen. 2006. The influence of advection on zooplankton community composition in an Arctic fjord (Kongsfjorden, Svalbard). J. Mar. Syst. **61**: 39–54. doi:10.1016/j.jmarsys.2005.11.013

Yebra, L., C. Almeida, and S. Hernandez-Leon. 2005. Vertical distribution of zooplankton and active flux across an

anticyclonic eddy in the Canary Island waters. Deep-Sea Res. Part I **52**: 69–83. doi:10.1016/j.dsr.2004.08.010

Zhang, X. S., and H. G. Dam. 1997. Downward export of carbon by diel migrant mesozooplankton in the central equatorial Pacific. Deep-Sea Res. Part II Top. Stud. Oceanogr. **44**: 2191–2202. doi:10.1016/S0967-0645(97)00060-X

## Acknowledgments

We thank the crew of the R/V *Helmer-Hanssen* and *Teisten* as well as Kings Bay personnel in Ny-Ålesund and Daniel Vogedes for their precious assistance in logistics and sampling. This work would not have been possible without the help of Colin Griffiths, Estelle Dumont, Trine Callesen, Marit Reigstad, Marina Sanz-Martin, Catherine Lalande, Miriam Marquardt, Anna Vader, Carl Ballantine, Slawek Kwasniewski, and the students of AB320/820 zooplankton course in 2014 (Morgan Bender, Heather Cronin, Ursula Ecker, Maeve McGovern, Sam Eglund Newby, Erik Haar Nielsen, Alejandro Prat, Pierre Priou, Mie Lundfryd Rasmussen, Petra Svaskova, Lotte Devries, Séan Mac Siúlaí, Sören Häfker, Helena Michelsen, Marc Silberberger). We wish to thank Hauke Flores and an anonymous reviewer for providing useful comments that helped improve this work substantially. The study is a contribution to: two NRC funded projects, Circa (NRC project number 214271) and Marine Night (NRC project number 226417), the Norwegian Polar Institute project N-ICE, and the Fjord and Coast Flagship of the FRAM-High North Research Centre for Climate and the Environment.

## Conflict of Interest

None declared.

*Submitted 18 February 2016*
*Revised 22 November 2016*
*Accepted 04 January 2017*

*Associate editor: Anya Waite*